



HAL
open science

Spin Squeezing in Finite Temperature Bose-Einstein Condensates: Scaling with the system size

Alice Sinatra, Emilia Witkowska, Yvan Castin

► **To cite this version:**

Alice Sinatra, Emilia Witkowska, Yvan Castin. Spin Squeezing in Finite Temperature Bose-Einstein Condensates: Scaling with the system size. 2011. hal-00652808v1

HAL Id: hal-00652808

<https://hal.science/hal-00652808v1>

Preprint submitted on 16 Dec 2011 (v1), last revised 30 Apr 2012 (v2)

HAL is a multi-disciplinary open access archive for the deposit and dissemination of scientific research documents, whether they are published or not. The documents may come from teaching and research institutions in France or abroad, or from public or private research centers.

L'archive ouverte pluridisciplinaire **HAL**, est destinée au dépôt et à la diffusion de documents scientifiques de niveau recherche, publiés ou non, émanant des établissements d'enseignement et de recherche français ou étrangers, des laboratoires publics ou privés.

Spin Squeezing in Finite Temperature Bose-Einstein Condensates : Scaling with the system size

A. Sinatra,¹ E. Witkowska,² and Y. Castin¹

¹*Laboratoire Kastler Brossel, Ecole Normale Supérieure, UPMC and CNRS, Paris, France*

²*Institute of Physics, Polish Academy of Sciences, Warszawa, Poland*

(Dated: December 16, 2011)

We perform a multimode treatment of spin squeezing induced by interactions in atomic condensates, and we show that, at finite temperature, the maximum spin squeezing has a finite limit when the atom number $N \rightarrow \infty$ at fixed density and interaction strength. To calculate the limit of the squeezing parameter for a spatially homogeneous system we perform a double expansion with two small parameters: $1/N$ in the thermodynamic limit and the non-condensed fraction $\langle N_{\text{nc}} \rangle / N$ in the Bogoliubov limit. To test our analytical results beyond the Bogoliubov approximation, and to perform numerical experiments, we use improved classical field simulations with a carefully chosen cut-off, such that the classical field model gives for the ideal Bose gas the correct non-condensed fraction in the Bose-condensed regime.

PACS numbers: 03.75.Gg, 42.50.Dv, 03.75.Kk, 03.75.Pp, 03.75.Mn.

I. INTRODUCTION

A two-level atom can be described as an effective spin $1/2$. Here, to describe an ensemble of atoms in two different internal states a and b , that are typically two hyperfine states, we use the picture of a “collective spin”. This spin, of length $N/2$, is simply the sum of the effective spins $1/2$ that describe the internal degrees of freedom of each atom. In the second quantized formalism the three hermitian spin components \hat{S}_x , \hat{S}_y and \hat{S}_z are defined by:

$$\hat{S}_+ \equiv \hat{S}_x + i\hat{S}_y = \int d^3r \hat{\psi}_a^\dagger(\mathbf{r})\hat{\psi}_b(\mathbf{r}) \quad (1)$$

$$\hat{S}_z = \frac{\hat{N}_a - \hat{N}_b}{2} \quad (2)$$

where the bosonic field operators $\hat{\psi}_{a,b}$ obey the usual commutation relations, $\hat{N}_a = \int d^3r \hat{\psi}_a^\dagger(\mathbf{r})\hat{\psi}_a(\mathbf{r})$ is the atom number in component a and the same for b . The spin operators are dimensionless and obey the commutation relations $[\hat{S}_x, \hat{S}_y] = i\hat{S}_z$ and cyclic permutations. Physically \hat{S}_z is the population difference between a and b states, while \hat{S}_x and \hat{S}_y describe one-body coherence between them.

Spin squeezing [1] is about creating quantum correlations, in such an ensemble of atoms, that can be useful for metrology. In particular spin squeezed states can be used to improve the accuracy of atomic clocks beyond the so called “standard quantum limit” that has been already reached in the most precise clocks [2]. The resulting gain for metrology is quantified by a spin squeezing parameter ξ^2 [3, 4]:

$$\xi^2 = \frac{N\Delta S_{\perp,\min}^2}{|\langle \mathbf{S} \rangle|^2}, \quad (3)$$

where N is the total atom number and $\Delta S_{\perp,\min}^2$ is the minimal variance of the collective spin orthogonally to

the direction of its mean value $\langle \mathbf{S} \rangle$. The state is squeezed if and only if $\xi^2 < 1$. As explained in [3], in an atomic clock experiment using Ramsey population spectroscopy, ξ directly gives the reduction in the statistical fluctuations of the measured frequency ω_{ab} with respect to using uncorrelated atoms (for the same atom number N and the same Ramsey time \mathcal{T}):

$$\Delta\omega_{ab}^{\text{sq}} = \xi\Delta\omega_{ab}^{\text{unc}} = \frac{\xi}{\sqrt{N\mathcal{T}}} \quad (4)$$

The parameter ξ in Eq.(3) is in fact the properly normalized ratio between the “noise” $\Delta S_{\perp,\min}$ and the “signal” $|\langle \mathbf{S} \rangle|$. In experiments $\Delta S_{\perp,\min}$ is directly measured by measuring \hat{S}_z after an appropriate state rotation and $|\langle \mathbf{S} \rangle|$ is separately deduced from the Ramsey fringes contrast.

Very recently experimental breakthroughs in spin squeezing have been achieved using either the interaction between atoms and light in an optical cavity [5] or atomic interactions in bimodal Bose-Einstein condensates [6], [7]. The ultimate limits of the different paths to spin squeezing are still objects of active studies [8–12]. We address here the issue of non-zero temperature and of the influence of the non condensed fraction for spin squeezing schemes using Bose-Einstein condensates.

We face the following physical problem: An interacting Bose gas, prepared at finite temperature in the internal state a , is subjected to a sudden $\pi/2$ mixing pulse that puts each atom in a coherent superposition of two different internal states a and b . From this out of equilibrium state, with factorized spin and motional variables, quantum correlations and spin squeezing are created dynamically by the atomic interactions [1], [4]. Let us first sketch how this happens in a simple two-mode picture, i.e. assuming that all the atoms in a or b share the same wave function for their motional degrees of freedom. After the mixing pulse, the two condensates in a and b have a well defined relative phase, with a relative phase

distribution whose width scales as $1/\sqrt{N}$, and fluctuations in the relative particle number difference scaling as \sqrt{N} . In a two-mode picture, the initial state can be expanded over Fock states $|N_a, N - N_a\rangle$ with N_a particles in state a and $N - N_a$ particles in state b . Due to atom-atom interactions, each Fock state acquires a phase in the evolution that is proportional to $N_a - N_b$ [1, 13, 14]. This situation is completely equivalent to the evolution of a coherent state in a Kerr medium in optics. During the evolution, due to the different phase shifts of the different Fock states, the relative phase distribution starts to spread. At the same time, quantum fluctuations orthogonal to the mean spin direction get distorted and, before the relative phase distribution has sensibly spread, spin squeezing is created in the sample. Our aim is to include the two-mode quantum dynamics that we just described, *and* the effect of the thermally excited non-condensed modes *within the same formalism*. The thermal modes *also* provide a condensate phase spreading [15],[16],[17],[18] and are expected to affect the spin squeezing generated in the system at non-zero temperature [9]. For a review of spin squeezing and decoherence see also [11].

A central issue is the *scaling of the squeezing* as the system gets large, i.e. in the thermodynamic limit. Most studies are based on a two-mode description [1]. In this frame the squeezing parameter minimized over time ξ_{\min}^2 tends to zero (infinite metrology gain) for $N \rightarrow \infty$ as $\xi_{\min}^2 \sim N^{-2/3}$. Although some studies beyond the two-mode theory were performed [4, 19, 20] they could not prove or disprove the two-mode scaling of spin squeezing in real condensates. Here we can go further. We find that for realistic atom numbers, the two-mode scaling $\xi_{\min}^2 \sim N^{-2/3}$ is meaningless at finite temperature and that the spin squeezing parameter ξ_{\min}^2 at the thermodynamic limit has a finite non-zero value that we calculate explicitly. In this paper we present a detailed derivation of the results given in [9] and we present new improved classical field simulations, with a carefully chosen cut-off such that the classical field model gives for the ideal Bose gas the correct non-condensed fraction in the Bose-condensed regime. We also present results for the squeezing that would be measured by detecting only the condensed particles, which we call the “condensate squeezing”, and we show that it is much worse than the squeezing of the total field for reasons that we explain in the paper.

In section II we formalize the problem and expose our approach to solve it. In section III we proceed with two numerical experiments. These experiments show (i) the existence of a non-zero thermodynamic limit for the squeezing parameter in contrast with the predictions of the two-mode theory, and (ii) the universal scaling with the temperature of the squeezing in the thermodynamic and weakly interacting limit. Analytical calculations are performed in section IV. By performing a double expansion of ξ_{\min}^2 in terms of two small parameters, the inverse atom number $1/N$ controlling the thermody-

amic limit and the non-condensed fraction controlling the weakly interacting limit, we obtain explicitly the minimal squeezing parameter that it is possible to achieve by this method as a function of the initial temperature and the interaction strength. A physical interpretation of the results is given in section V. In that section we also show that the squeezing defined for the total field and the squeezing defined for the condensate mode only are very different and we give a physical explanation. We conclude in section VI.

II. THE PROBLEM

A. The Quantum Model

We consider a spatially homogeneous system of N bosons in two internal states that interact with short range binary interactions. We take for simplicity identical interactions in components a and b and no crossed a - b interactions [36]. The system is discretized on a cubic lattice of lattice spacing l , with periodic boundary condition of period L along each direction x, y, z . For numerical convenience, $L/l = n_{\max}$ is an even integer. There are in total $\mathcal{N} \equiv V/dV$ lattice points, where $V = L^3$ is the system volume and $dV = l^3$ the unit cell volume. The Hamiltonian for one separate spin component, e.g. component a , reads

$$\hat{H}_a = \sum_{\mathbf{k}} \frac{\hbar^2 k^2}{2m} \hat{a}_{\mathbf{k}}^\dagger \hat{a}_{\mathbf{k}} + \frac{g_0}{2} dV \sum_{\mathbf{r}} \hat{\psi}_a^\dagger(\mathbf{r}) \hat{\psi}_a^\dagger(\mathbf{r}) \hat{\psi}_a(\mathbf{r}) \hat{\psi}_a(\mathbf{r}) \quad (5)$$

In the kinetic energy term we have expanded the field operator over plane waves

$$\hat{\psi}_a(\mathbf{r}) = \sum_{\mathbf{k}} \hat{a}_{\mathbf{k}} \frac{e^{i\mathbf{k}\cdot\mathbf{r}}}{\sqrt{V}} \quad (6)$$

and $\hat{a}_{\mathbf{k}}$ annihilates a particle of wave vector \mathbf{k} belonging to the first Brillouin zone (FBZ) $[-\pi/l, \pi/l]^3$ of the lattice, so that along each direction ν , $k_\nu \in \frac{2\pi}{L} \{-L/(2l), \dots, L/(2l) - 1\}$. Since we consider a lattice model, the field operator here obeys the discrete bosonic commutation relations (A1). The second term in (5) represents atomic interactions modeled by a purely on-site interaction with a bare coupling constant on the lattice g_0 . In practice, to recover the continuous space physics, l is taken to be smaller than both the healing length ξ and the thermal de Broglie wavelength λ_{dB} . In the weakly interacting regime, $|a| \ll \xi, \lambda_{\text{dB}}$, one can further take $l \gg |a|$ so that in the following we will identify g_0 with the effective coupling constant $g = 4\pi\hbar^2 a/m$ where a is the s -wave scattering length [37].

Initially at $t < 0$, all the N atoms are in the internal state a in thermal equilibrium described by the canonical density operator

$$\hat{\rho} = \frac{1}{Z} e^{-\beta \hat{H}_a} \quad (7)$$

with $\beta = 1/(k_B T)$ and $T \ll T_c$ where T_c is the transition temperature for Bose-Einstein condensation.

At $t = 0$ an electromagnetic pulse mixes the states a and b . The pulse Hamiltonian acting during a time interval t_{pulse} is

$$\hat{V}_p = \frac{\hbar\Omega}{2i} \sum_{\mathbf{r}} dV (\hat{\psi}_a^\dagger \hat{\psi}_b - \hat{\psi}_b^\dagger \hat{\psi}_a) \quad (8)$$

In practice the timescale t_{pulse} is shorter than all the relevant timescales in the original Hamiltonians $H_{a,b}$ so that we can take the limit $t_{\text{pulse}} \rightarrow 0$, $\Omega \rightarrow \infty$ with $\Omega t_{\text{pulse}} = \pi/2$. After integration of the Heisenberg equations of motion during t_{pulse} , it is found that the fields are transformed by the $\pi/2$ pulse as follows:

$$\hat{\psi}_a(0^+) = \frac{1}{\sqrt{2}} [\hat{\psi}_a(0^-) - \hat{\psi}_b(0^-)] \quad (9)$$

$$\hat{\psi}_b(0^+) = \frac{1}{\sqrt{2}} [\hat{\psi}_a(0^-) + \hat{\psi}_b(0^-)] \quad (10)$$

We are interested in the squeezing and quantum correlations that develop during the non-equilibrium dynamics following the pulse for $t > 0$.

B. Our Approach

The problem of the scaling of the squeezing for $N \rightarrow \infty$ in the multimode case implies the solution of the non-equilibrium quantum dynamics for a large number of atoms and a large number of modes. We cannot solve exactly this problem even numerically. However, what can be solved exactly on a computer is the ‘‘classical field equivalent’’ of our problem. We then adopt the strategy summarized in Table I. We use the classical field model to (i) perform numerical experiments and (ii) test a perturbative solution that we can generalize to the quantum case. The quantum perturbative solution is then used to get quantitative predictions on the real physical system.

Quantum field model	solution available ?	Classical field model	solution available ?
$\hat{H}[\hat{\psi}_a(\mathbf{r}), \hat{\psi}_b(\mathbf{r})]$	no	$H[\psi_a(\mathbf{r}), \psi_b(\mathbf{r})]$	yes
			\updownarrow
Perturbative	yes	Perturbative	yes

TABLE I: We cannot solve exactly the problem in the quantum case but we find an analytical perturbative solution. We check our perturbative approach in the classical case where we can solve the model exactly (numerically).

C. Classical field model

The classical field model [21, 22] is obtained by replacing the quantum fields with classical fields in the

Hamiltonian[38]

$$\hat{\psi}_a^\dagger, \hat{\psi}_a, \hat{\psi}_b^\dagger, \hat{\psi}_b \rightarrow \psi_a^*, \psi_a, \psi_b^*, \psi_b. \quad (11)$$

In the equations of motion the commutators are then replaced by Poisson brackets. The classical field model is useful when the interesting physics is given by low-energy highly populated modes [23–25]. For our classical field simulations, we assume that this is the case in the equilibrium state before the pulse, with all the particles in state a . The initial field $\psi_a^{(0)}$ then randomly samples the thermal equilibrium classical field distribution for the canonical ensemble at temperature T

$$\rho_{\text{cl}} = \frac{1}{Z} e^{-\beta H} \quad (12)$$

where H is the classical Hamiltonian, which is a discrete version of the Gross-Pitaevskii energy functional:

$$H = \sum_{\mathbf{k}} \frac{\hbar^2 k^2}{2m} a_{\mathbf{k}}^* a_{\mathbf{k}} + \frac{g}{2} dV \sum_{\mathbf{r}} \psi_a^*(\mathbf{r}) \psi_a^*(\mathbf{r}) \psi_a(\mathbf{r}) \psi_a(\mathbf{r}) \quad (13)$$

For the initially empty state b , inspired by the Wigner quasi-probability distribution of the quantum density operator and the truncated Wigner approach [26–29] we represent the vacuum by a classical field $\psi_b^{(0)}$ having in each mode independent Gaussian complex fluctuations of zero mean and variance $1/2$: More precisely, we set $b_{\mathbf{k}}^{(0)} = X + iY$ where the independent real random variables X and Y have the same Gaussian probability distribution

$$P(x) = \sqrt{\frac{2}{\pi}} e^{-2x^2} \quad (14)$$

At $t = 0$ the fields are mixed by the pulse according to (9)-(10). At later times, the fields, ψ_a and ψ_b evolve independently according to the discrete non-linear Schrödinger equation ($\nu = a, b$)

$$i\hbar \partial_t \psi_\nu = \left[-\frac{\hbar^2 \Delta}{2m} + g |\psi_\nu(\mathbf{r}, t)|^2 \right] \psi_\nu \quad (15)$$

where the discrete Laplacian Δ has the plane waves $\exp(i\mathbf{k} \cdot \mathbf{r})$ on the lattice as eigenvectors of eigenvalues $-k^2$. The lattice model automatically provides a momentum cut-off to the classical field model, corresponding to the boundaries of the first Brillouin zone $\text{FBZ} = [-\pi/l, \pi/l]^3$. The various observables have a more or less pronounced dependence on the cut-off. Here, guided by our analytical results (see section IV) we choose the cut-off such that, in the thermodynamic limit, the non-condensed density for an ideal continuous space gas in the Bose condensed regime (zero chemical potential) is exactly reproduced by the classical field model:

$$\int_{\mathbb{R}^3} \frac{d^3 k}{(2\pi)^3} \frac{1}{e^{\beta E_k} - 1} = \int_{\text{FBZ}} \frac{d^3 k}{(2\pi)^3} \frac{k_B T}{E_k} \quad (16)$$

where $E_k = \hbar^2 k^2 / 2m$ is the kinetic energy, the mode occupation numbers are given by the Bose formula for the quantum case and by the equipartition formula for the classical case. The condition (16) is an equation for l/λ_{dB} with the thermal de Broglie wavelength $\lambda_{\text{dB}} = [2\pi\hbar^2/(mk_B T)]^{1/2}$, as is revealed by the change of integration variable $\mathbf{K} = \lambda_{\text{dB}} \mathbf{k}$. The integrals on both sides of (16) can be calculated analytically, see e.g. [30] for the integral in the right-hand side, and the usual factor $\zeta(3/2)$ appears in the left-hand side (where ζ is the Riemann Zeta function). The condition (16) then gives $E_k^{\text{max}} \simeq 2.695 k_B T$ with E_k^{max} is the maximal kinetic energy on the grid, here $E_k^{\text{max}} = 3\hbar^2(\pi/l)^2/(2m)$ [39].

III. NUMERICAL EXPERIMENTS

A. Dimensional analysis

As specified in subsection II A, when the lattice model approaches the continuous space physics for the spin squeezing, the physical parameters of the model are the atom mass m , the effective coupling constant g characterizing low energy binary interactions between the atoms, the temperature T , the total atom number N and system volume V :

$$\frac{\hbar^2}{m}, g, k_B T, N, V \quad (17)$$

The spin squeezing parameter optimized over time, ξ_{min}^2 , is a dimensionless quantity. It is therefore a function of the independent dimensionless combinations that we can form from the ensemble (17):

$$\xi_{\text{min}}^2 = f\left(N, \sqrt{\rho a^3}, \frac{k_B T}{\rho g}\right) \quad (18)$$

Here $\sqrt{\rho a^3}$ is the ‘‘small parameter’’ such that $\sqrt{\rho a^3} \ll 1$ characterizes the weakly interacting limit, and ρg is the mean field chemical potential of the gas (at $T = 0$). The same dimensional analysis and the same general form of ξ_{min}^2 hold for the classical field model.

B. Existence of a thermodynamic limit for ξ^2

We have performed classical field simulations, increasing the system size in the thermodynamic limit

$$N \rightarrow \infty; V \rightarrow \infty; \rho, g, T = \text{constant}, \quad (19)$$

In Fig.1 we show the result for four different temperatures. The squeezing parameter, minimized over time, converges to a finite value. According to the general form (18), ξ_{min}^2 then depends on $k_B T/\rho g$ and $\sqrt{\rho a^3}$. The first parameter $k_B T/\rho g$ is varied in Fig.1, whereas the parameter $\sqrt{\rho a^3}$ defining the weakly interacting regime is maintained constant in that figure. Note that for curves

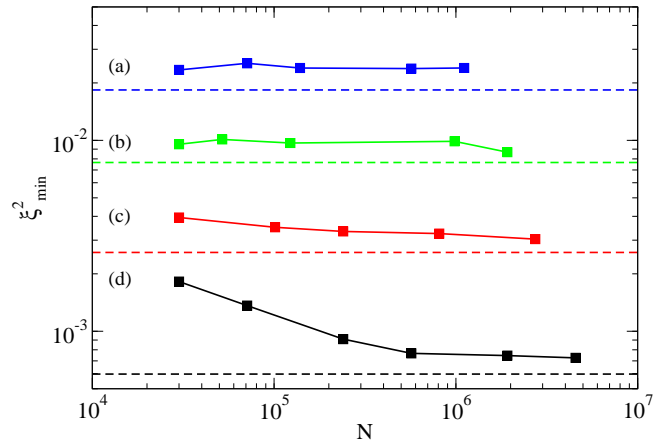


FIG. 1: (Color online). Minimal squeezing parameter (that is, minimized over time) for four different temperatures and increasing system sizes in the thermodynamic limit $N \rightarrow \infty$, $\rho, g, T = \text{constant}$. Squares: classical field simulations result. $k_B T/\rho g = 1.13(a), 0.78(b), 0.50(c), 0.28(d)$. For all the points $\sqrt{\rho a^3} = 1.32 \times 10^{-2}$. The horizontal dashed lines are analytical results in the thermodynamic and weakly interacting limit (21) that are the classical field equivalent of (62). The grid sizes (number of points per direction) are $n_{\text{max}} = 12, 16, 20, 32, 36$ for (a), $n_{\text{max}} = 10, 12, 16, 32, 40$ for (b), $n_{\text{max}} = 12, 16, 24, 36, 40$ for (c) and $n_{\text{max}} = 6, 8, 12, 16, 24, 32$ for (d).

(a)-(c) the limit is already almost reached for $N = 3 \times 10^4$ while a larger system is needed for the lowest temperature curve (d).

C. Weakly interacting limit of ξ^2

Starting from a point that is already at the thermodynamic limit for each temperature, we have performed other simulations, going more deeply in the weakly interacting limit $\rho \rightarrow \infty, g \rightarrow 0, \rho g, T = \text{constant}$ [31] [40]. In this limit the small parameter $\sqrt{\rho a^3}$ tends to zero. In Fig.2, for a fixed value of $k_B T/\rho g$, we show the squeezing parameter divided by $\sqrt{\rho a^3}$ as a function of a rescaled time, for various values of $\sqrt{\rho a^3}$. It is apparent that the rescaled minimal squeezing is nearly constant in the figure. For weak interactions, $\xi_{\text{min}}^2/\sqrt{\rho a^3}$ is thus a function of $k_B T/\rho g$ only.

D. Spin squeezing as a function of the temperature

From the numerical experiments described in III B and III C, we conclude that, in the double thermodynamic plus weakly interacting limit, the squeezing parameter minimized over time is equal to $\sqrt{\rho a^3}$ times a universal function of $k_B T/\rho g$:

$$\xi_{\text{min}}^2 = \sqrt{\rho a^3} F\left(\frac{k_B T}{\rho g}\right) \quad (20)$$

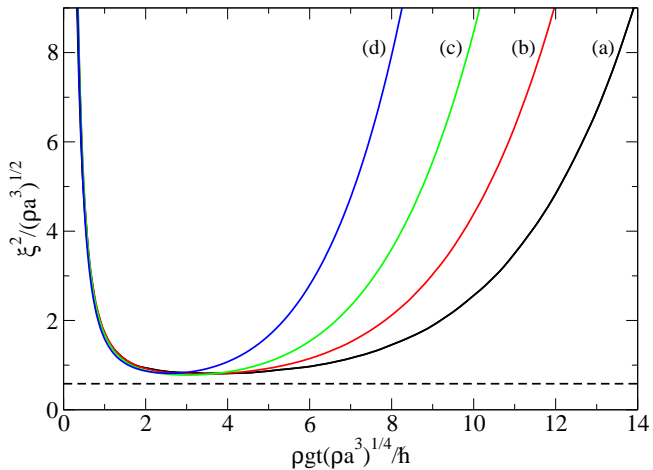


FIG. 2: (Color online). Squeezing parameter ξ^2 divided by $\sqrt{\rho a^3}$ as a function of a rescaled time, in the weakly interacting limit: $\rho \rightarrow \infty$, $g \rightarrow 0$ with $\rho g, T = \text{constant}$. Solid lines: classical field simulations. Parameters: $k_B T / \rho g = 0.5$ and $n_{\text{max}} = 32$ for all the curves. (a) $N = 3 \times 10^4$, $\sqrt{\rho a^3} = 1.32 \times 10^{-2}$; (b) $N = 10^5$, $\sqrt{\rho a^3} = 3.96 \times 10^{-3}$; (c) $N = 3 \times 10^5$, $\sqrt{\rho a^3} = 1.32 \times 10^{-3}$; (d) $N = 6 \times 10^5$, $\sqrt{\rho a^3} = 6.59 \times 10^{-4}$. Horizontal line: analytical result (21).

We show the universal scaling of the minimal squeezing parameter in the thermodynamic limit in Fig.3, where we collect the results of several simulations for different temperatures and interaction strengths. In the following section we shall develop the analytical theory that gives the explicit expression of the function F appearing in (20). The analytical result for the classical field theory is represented as a full line in Fig.3. It reads:

$$\xi_{\text{min}}^2 = \int_{\text{FBZ}} \frac{d^3 k}{(2\pi)^3} \frac{s_k^4}{2\rho} n_k^{(0)} \left(\frac{(s_k^{(0)})^2}{s_k^4} + \frac{s_k^4}{(s_k^{(0)})^2} \right) \quad (21)$$

Here $\rho = N/V$ is the total density, $s_k = U_k + V_k$, $s_k^{(0)} = U_k^{(0)} + V_k^{(0)}$ are Bogoliubov functions defined in (30) and (28), $n_k^{(0)} = k_B T / \epsilon_k^{(0)}$ are the equilibrium occupation numbers of Bogoliubov modes before the pulse with $\epsilon_k^{(0)} = [E_k(E_k + 2\rho g)]^{1/2}$ and the integral is restricted to the first Brillouin zone FBZ with $k_\nu \in [-k_\nu^{\text{max}}, k_\nu^{\text{max}}]$ for the three directions $\nu = x, y, z$. We note a very good agreement between the analytics and the simulations for all the points. For comparison, we also show the analytical result for the quantum field (62), in the zero-lattice spacing limit, as a dashed line. Note how well the classical results with the cut-off prescription (16) reproduce the quantum analytical results for $k_B T > \rho g$.

IV. ANALYTICAL RESULTS

We want here to address the fully quantum case and calculate analytically the function $F(k_B T / \rho g) =$

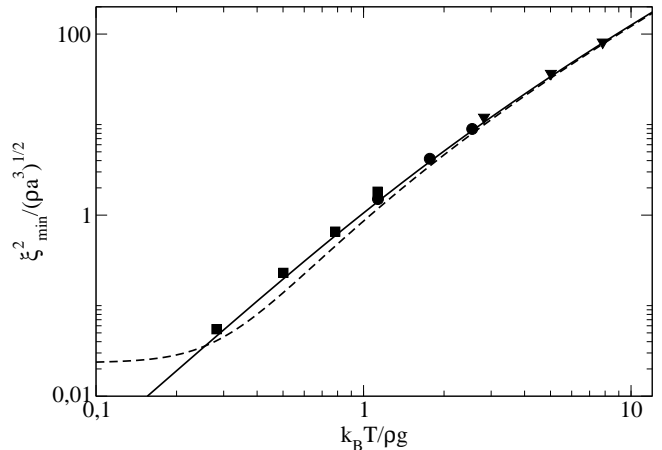


FIG. 3: Minimal squeezing parameter ξ_{min}^2 divided by $\sqrt{\rho a^3}$ as a function of $k_B T / \rho g$. Symbols: classical field simulations with $\sqrt{\rho a^3} = 1.32 \times 10^{-2}$ (squares), 1.94×10^{-3} (disks), and $\sqrt{\rho a^3} = 4.17 \times 10^{-4}$ (triangles). Solid line: Analytical classical field result (21). Dashed line: Quantum result (62). The grid sizes, for increasing $k_B T / \rho g$ are $n_{\text{max}} = 32, 36, 40, 36$ for squares, $n_{\text{max}} = 24, 32, 32$ for disks and $n_{\text{max}} = 32$ for triangles. The initial non condensed fractions in component a before the pulse are $\langle N_{\text{nc}} \rangle / N = 0.01, 0.02, 0.04, 0.07$ for squares, $\langle N_{\text{nc}} \rangle / N = 0.01, 0.02, 0.04$ for disks and $\langle N_{\text{nc}} \rangle / N = 0.01, 0.02, 0.05$ for triangles.

$\xi_{\text{min}}^2 / \sqrt{\rho a^3}$ of (20) using Bogoliubov theory. In IV A we present a modulus-phase reformulation of the Bogoliubov theory generalized for a bimodal condensate; in IV B and IV C we derive the expansion of the spin squeezing parameter in the thermodynamic limit, and we discuss the final analytical results in IV D.

A. Modulus-phase Bogoliubov formalism for bimodal condensates

We generalize here to two-components the $U(1)$ -symmetry preserving Bogoliubov theory of [31], see also [4]. As spin squeezing in bimodal condensates is due to phase dynamics, we rephrase the theory in terms of the relative phase operator of the a and b condensates. This is a crucial step that allows us to obtain results by a perturbative expansion in powers of that relative phase. The relative phase is simply the difference of the condensate phases $\hat{\theta}_{a,b}$ introduced as hermitian operators conjugate to the condensate atom numbers [32, 33]. This is a valid description in the subspace excluding the vacuum state (no particles) for the condensate modes, which is sufficient here: as we suppose initially $T \ll T_c$, both condensates are highly populated after the mixing pulse with $\langle N_a \rangle = \langle N_b \rangle = N/2$. Some useful expressions involving the Bogoliubov amplitudes and some commutation relations are given in Appendix A.

Within each atomic internal state a or b , we split the bosonic field operator into the condensate and non con-

densed modes contributions:

$$\hat{\psi}_a = \frac{\hat{a}_0}{\sqrt{V}} + \hat{\psi}_{a\perp}, \quad \hat{\psi}_b = \frac{\hat{b}_0}{\sqrt{V}} + \hat{\psi}_{b\perp} \quad (22)$$

For the annihilation operators in the condensate modes we introduce the modulus-phase representation

$$\hat{a}_0 = e^{i\hat{\theta}_a} \sqrt{\hat{N}_{a0}}, \quad [\hat{N}_{a0}, \hat{\theta}_a] = i \quad (23)$$

$$\hat{b}_0 = e^{i\hat{\theta}_b} \sqrt{\hat{N}_{b0}}, \quad [\hat{N}_{b0}, \hat{\theta}_b] = i, \quad (24)$$

while for the non condensed modes we introduce the number conserving fields [31, 34]

$$\hat{\Lambda}_a = e^{-i\hat{\theta}_a} \hat{\psi}_{a\perp}; \quad \hat{\Lambda}_b = e^{-i\hat{\theta}_b} \hat{\psi}_{b\perp} \quad (25)$$

that we expand over Bogoliubov modes with amplitudes $\hat{c}_{a\mathbf{k}}$ and $\hat{c}_{b\mathbf{k}}$. To perform this expansion, one has to distinguish the time before the pulse and the time after the pulse.

Before the pulse, at time $t = 0^-$, all the N atoms are in the internal state a , with a zero-temperature mean field chemical potential $\mu = \rho g$, and we expand the number conserving field $\hat{\Lambda}_a(t = 0^-)$ over the Bogoliubov modes:

$$\hat{\Lambda}_a^{(0)} = \sum_{\mathbf{k} \neq 0} \left[U_k^{(0)} \hat{c}_{a\mathbf{k}}^{(0)} + V_k^{(0)} (\hat{c}_{a-\mathbf{k}}^{(0)})^\dagger \right] \frac{e^{i\mathbf{k}\cdot\mathbf{r}}}{\sqrt{V}} \quad (26)$$

Here the exponent (0) over the operators indicates that the operators are considered at time $t = 0^-$. The bosonic operator $\hat{c}_{a\mathbf{k}}^{(0)}$ annihilates a Bogoliubov quasi-particle of wave vector \mathbf{k} , and eigenenergy

$$\epsilon_k^{(0)} = [E_k(E_k + 2\rho g)]^{1/2} \quad (27)$$

where we recall that $E_k = \hbar^2 k^2 / (2m)$ is the kinetic energy contribution. The corresponding amplitudes of the Bogoliubov mode, correctly normalized as $[U_k^{(0)}]^2 - [V_k^{(0)}]^2 = 1$, are given by

$$s_k^{(0)} \equiv U_k^{(0)} + V_k^{(0)} = \frac{1}{U_k^{(0)} - V_k^{(0)}} = \left(\frac{E_k}{E_k + 2\rho g} \right)^{1/4} \quad (28)$$

Before the pulse, the field in the b state is in the vacuum state, so the modal expansion is performed over the usual single particle plane wave eigenbasis.

After the pulse, at $t \geq 0^+$, the particles are on average equally distributed among the two internal states a and b , $\langle N_a \rangle = \langle N_b \rangle = N/2$. There are now two condensates, with interaction constants $g_{aa} = g_{bb} = g$ among atoms of same internal state, and no interaction ($g_{ab} = 0$) among atoms of different internal states. Similarly to (26), we perform after the pulse the modal decomposition of the number conserving fields in each internal state $\sigma = a, b$:

$$\hat{\Lambda}_\sigma = \sum_{\mathbf{k} \neq 0} \left[U_k \hat{c}_{\sigma\mathbf{k}} + V_k \hat{c}_{\sigma-\mathbf{k}}^\dagger \right] \frac{e^{i\mathbf{k}\cdot\mathbf{r}}}{\sqrt{V}} \quad (29)$$

where $\hat{c}_{\sigma\mathbf{k}}$ annihilates a Bogoliubov quasi-particle of wave vector \mathbf{k} in internal state σ . The Bogoliubov mode amplitudes U_k, V_k and the eigenenergies ϵ_k do not depend on the internal state and are deduced from the ones at $t = 0^-$ by replacing the mean field term ρg by $\rho g/2$:

$$s_k \equiv U_k + V_k = \frac{1}{U_k - V_k} = \left(\frac{E_k}{E_k + \rho g} \right)^{1/4} \quad (30)$$

$$\epsilon_k = [E_k(E_k + \rho g)]^{1/2}, \quad (31)$$

Note that this involves an approximation: In principle, the Bogoliubov modes in internal state $\sigma = a$ or b depend on the actual number of particles N_σ in that state, which has small $\approx 1/\sqrt{N}$ relative fluctuations since, after the pulse, N_σ has a binomial distribution peaked around $N/2$. Taking into account this effect changes the mathematical structure of the theory, since the Bogoliubov amplitudes U_k and V_k , and thus the quasi-particle annihilation operators $\hat{c}_{\sigma\mathbf{k}}$, would then depend on the total number operator \hat{N}_σ in state σ , which is beyond the scope of the present work. We nevertheless verified numerically on the complete Bogoliubov theory (in the classical field model) that this fixed-Bogoliubov-mode approximation is extremely accurate both at short and long times, introducing (for the typical parameters considered in our figures) a relative error on ξ^2 lower than 10^{-2} comparable to our statistical error bars with 10^5 realizations. Another important point is that the Bogoliubov quasi-particles are not at thermal equilibrium after the pulse, so that, for example, their mean occupation numbers are not given by the Bose formula. At the level of the Bogoliubov approximation, the quasi-particles do not interact and cannot thermalize, the corresponding quasi-particle creation operators evolve in Heisenberg picture with simple phase factors:

$$\hat{c}_{\sigma\mathbf{k}}(t) \underset{t>0}{=} e^{-i\epsilon_k t/\hbar} \hat{c}_{\sigma\mathbf{k}}(0^+) \quad (32)$$

for $\sigma = a, b$. The validity of this no-thermalization approximation is discussed in subsection IV D.

To express the evolution of the particle annihilation operators \hat{a}_0 and \hat{b}_0 in the condensate modes, we use the modulus-phase representation (23, 24). For the modulus, one simply uses the conservation of the total atom number in each internal state,

$$\hat{N}_{\sigma 0} = \hat{N}_\sigma - \hat{N}_{\sigma\perp} = \hat{N}_\sigma - \sum_{\mathbf{r}} dV \hat{\Lambda}_\sigma^\dagger \hat{\Lambda}_\sigma \quad (33)$$

so that $\hat{N}_{\sigma 0}$ can be expressed in terms of the quasi-particle operators $\hat{c}_{\sigma\mathbf{k}}$. For the phase, we use within each internal state $\sigma = a, b$ the equation of motion derived for a single component in [16] and truncated at the level of the Bogoliubov approximation:

$$\frac{d}{dt} \hat{\theta}_\sigma = -\chi \left(\hat{N}_\sigma - \frac{1}{2} \right) - \frac{\chi}{2} \sum_{\mathbf{r}} dV \left(\hat{\Lambda}_\sigma^2 + 2\hat{\Lambda}_\sigma^\dagger \hat{\Lambda}_\sigma + \hat{\Lambda}_\sigma^{\dagger 2} \right) \quad (34)$$

where we have introduced $\chi \equiv g/(\hbar V)$. Replacing the operators $\hat{\Lambda}_\sigma$ by their modal expansion (29), one gets contributions that do not oscillate in time, and contributions such as $\hat{c}_{\sigma\mathbf{k}}\hat{c}_{\sigma-\mathbf{k}}$ that oscillate in time (at the frequency $2\epsilon_{\mathbf{k}}/\hbar$ in the example). As we shall need the value of the phase operators at long times t (typically $\epsilon_{\mathbf{k}}t/\hbar \gg 1$) rather than the value of its derivative, we argue as in [16] that the oscillating terms in (34), after temporal integration, give a negligible contribution to the squeezing parameter. We have checked this approximation analytically: The expression for ξ^2 fully including the oscillating terms in the phase difference operator is given in the Appendix E, it corrects the approximate expression (60) of ξ^2 by typically a sub-percent effect at intermediate times, and by a vanishing amount at large times. These oscillating terms in $\hat{\theta}_a - \hat{\theta}_b$ are thus of little physical relevance for the spin squeezing. Keeping only the non-oscillating terms gives for the relative phase operator of the two condensates at time t :

$$(\hat{\theta}_a - \hat{\theta}_b)(t) = (\hat{\theta}_a - \hat{\theta}_b)(0^+) - \chi t \left[\hat{N}_a - \hat{N}_b + \hat{\mathcal{D}} \right] \quad (35)$$

$$\hat{\mathcal{D}} = \sum_{\mathbf{k} \neq 0} (U_{\mathbf{k}} + V_{\mathbf{k}})^2 (\hat{n}_{a\mathbf{k}} - \hat{n}_{b\mathbf{k}})(0^+) \quad (36)$$

where we have introduced the quasi-particle number operators $\hat{n}_{\sigma\mathbf{k}} = \hat{c}_{\sigma\mathbf{k}}^\dagger \hat{c}_{\sigma\mathbf{k}}$, which are constants of motion in the Bogoliubov approximation, see (32). The multimode contribution $\hat{\mathcal{D}}$ (36) to the relative phase (35) will play a central role in what follows. It is indeed because of this term (neglected in the usual two-mode models) that the squeezing parameter is bounded from below by a non-zero value in the thermodynamic limit.

The last step is to relate the various operators at time $t = 0^+$ to their values just before the pulse. Since the state of the system is known at $t = 0^-$, this fully specifies the ‘‘initial’’ conditions for the time evolution of the operators after the pulse. The derivation and the more precise results are given in the Appendix B. Here we give the main conclusions. The initial value of the condensate phase difference is, in the large N limit:

$$(\hat{\theta}_a - \hat{\theta}_b)(0^+) = \frac{i}{2} \left\{ \left(\hat{N}_{a0}^{(0)} \right)^{-1/2}, \left(\tilde{b}_0^{(0)} - \text{h.c.} \right) \right\} + O\left(\frac{1}{N^{3/2}}\right) \quad (37)$$

where $\tilde{b}_0^{(0)} \equiv e^{-i\theta_a^{(0)}} \hat{b}_0^{(0)}$ and $\{ , \}$ stands for the anticommutator. This results from the coherent mixing of the initial condensate amplitude with the vacuum noise fluctuations in the initially empty internal state b , in the same spatial mode as the initial condensate in state a , that is in the plane wave with zero wave vector. Similarly, the quasi-particle annihilation operators just after the pulse are coherent superpositions of the initial field fluctuations, mainly thermal fluctuations \hat{A} in a and only vacuum fluctuations \hat{B} in b . In the large N limit,

$$c_{\sigma\mathbf{k}}(0^+) = \frac{\hat{A}_{\mathbf{k}} \mp \hat{B}_{\mathbf{k}}}{\sqrt{2}} + O\left(\frac{1}{N^{1/2}}\right) \quad (38)$$

where the $-$ sign is for $\sigma = a$ and the $+$ sign is for $\sigma = b$. The expression of $\hat{A}_{\mathbf{k}}$ in terms of $t = 0^-$ operators of the a internal state, and the expression of $\hat{B}_{\mathbf{k}}$ in terms of $t = 0^-$ operators of the b internal state, naturally appear in the calculations of Appendix B:

$$\hat{A}_{\mathbf{k}} \equiv (U_{\mathbf{k}} U_{\mathbf{k}}^{(0)} - V_{\mathbf{k}} V_{\mathbf{k}}^{(0)}) c_{a\mathbf{k}}^{(0)} + (U_{\mathbf{k}} V_{\mathbf{k}}^{(0)} - V_{\mathbf{k}} U_{\mathbf{k}}^{(0)}) c_{a-\mathbf{k}}^{(0)\dagger} \quad (39)$$

$$\hat{B}_{\mathbf{k}} \equiv U_{\mathbf{k}} e^{-i\hat{\theta}_a^{(0)}} \hat{b}_{\mathbf{k}}^{(0)} - V_{\mathbf{k}} e^{i\hat{\theta}_a^{(0)}} \hat{b}_{-\mathbf{k}}^{(0)\dagger} \quad (40)$$

In Appendix C, it is pointed out that these number conserving operators obey bosonic commutation relations and all their second moments are explicitly evaluated.

B. Double expansion method in the thermodynamic and weakly interacting limit

We shall now apply the Bogoliubov theory developed in section IV A to the calculation of the time-dependent squeezing parameter ξ^2 defined in (3). For the configuration that we consider, symmetric under the exchange of a and b , the mean spin is always aligned along x . The minimum transverse spin variance is then

$$\Delta S_{\perp, \min}^2 = \frac{1}{2} \left[\langle \hat{S}_y^2 \rangle + \langle \hat{S}_z^2 \rangle - \sqrt{(\langle \hat{S}_y^2 \rangle - \langle \hat{S}_z^2 \rangle)^2 + \langle \{ \hat{S}_z, \hat{S}_y \} \rangle^2} \right], \quad (41)$$

where $\{ , \}$ is the anticommutator. From the definition (2) it appears that \hat{S}_z is a constant of motion, its variance can thus be evaluated just after the pulse, at $t = 0^+$. According to (9,10), the pulse applies to the collective spin a rotation of angle $\pi/2$ around y axis, so that

$$\hat{S}_z(t > 0) = -\hat{S}_x^{(0)} \quad \text{and} \quad \langle \hat{S}_z^2 \rangle = \frac{N}{4} \quad (42)$$

To obtain the spin variance $\langle \hat{S}_y^2 \rangle$ and the spin correlation $\langle \{ \hat{S}_y, \hat{S}_z \} \rangle$, the challenge is to determine, as a function of time, the operator \hat{S}_y , or equivalently the antihermitian part of the operator \hat{S}_+ introduced in (1) (in its discrete version for the lattice model), since $\hat{S}_y = (\hat{S}_+ - \text{h.c.})/(2i)$. In the expression of \hat{S}_+ , one applies the splitting (22) of the bosonic fields in the condensate and the non-condensed contributions, one uses the modulus-phase representation (23, 24) for the condensate part and one introduces the number-conserving fields $\hat{\Lambda}_\sigma$ for the non-condensed part, to obtain:

$$\hat{S}_+ = e^{-i(\hat{\theta}_a - \hat{\theta}_b)} \left(\frac{N}{2} + \hat{F} \right) \quad \text{with} \quad (43)$$

$$\hat{F} = \sqrt{(\hat{N}_{a0} + 1)\hat{N}_{b0}} - \frac{N}{2} + \sum_{\mathbf{r}} dV \hat{\Lambda}_a^\dagger \hat{\Lambda}_b \quad (44)$$

Guided by the numerical experiments in section III, we have developed a systematic *double expansion* technique

to determine $\langle \hat{S}_y^2 \rangle$ and $\langle \{\hat{S}_y, \hat{S}_z\} \rangle$. The two small parameters controlling the large system size limit [i.e. the thermodynamic limit (19)] and the Bogoliubov limit are

$$\epsilon_{\text{size}} = \frac{1}{N} \quad \text{and} \quad \epsilon_{\text{Bog}} \equiv \frac{\langle \hat{N}_{\text{nc}} \rangle}{N} \quad (45)$$

where $\langle \hat{N}_{\text{nc}} \rangle = \langle \hat{N}_{a\perp}^{(0)} \rangle$ is the mean number of non-condensed particles in the initial state, which is indeed much smaller than N for a weakly interacting gas at $T \ll T_c$. For the Bogoliubov expansion, we will keep terms up to order one included in ϵ_{Bog} ; keeping higher order terms would not be consistent with the use of the quadratic Bogoliubov Hamiltonian. To determine the required order of the large system size expansion, we note that $\langle \hat{S}_x \rangle$ in the denominator of (3) remains close to its $t = 0^+$ value $N/2$ over the relevant time scales (that are finite in the thermodynamic limit with $\rho g t / \hbar \ll N^{1/2}$), so that $\xi^2 \approx 4\Delta S_{\perp, \text{min}}^2 / N$. To have a vanishingly small error on ξ^2 in the thermodynamic limit, we will keep in $\langle \hat{S}_y^2 \rangle / N$ and $\langle \{\hat{S}_y, \hat{S}_z\} \rangle / N$ terms up to order zero included in ϵ_{size} , that is we can neglect the contributions that tend to zero when $\epsilon_{\text{size}} \rightarrow 0$.

The systematic technique to determine the order of an operator is to estimate its mean value and its standard deviation in the quantum state of the system. This is safer than a simple guess, in particular when the operator has a vanishing expectation value. A relevant example is the operator \hat{D} defined in (36), that will play a crucial role in the best achievable squeezing. After a superficial look at (36), one may believe that \hat{D} scales as N in the thermodynamic limit, since it involves a sum over all modes, and that it scales as ϵ_{Bog} in the Bogoliubov limit since it involves the quasi-particle number operators $\hat{n}_{\sigma\mathbf{k}}$. However, it is actually the differences $\hat{n}_{a\mathbf{k}} - \hat{n}_{b\mathbf{k}}$ that matter, and for the particular state resulting from a $\pi/2$ pulse applied on a gas initially in the a internal state. As a consequence, the expectation value of \hat{D} is zero, it is the variance of \hat{D} which scales as N , so \hat{D} scales as $N^{1/2}$ in the thermodynamic limit. To determine its scaling with ϵ_{Bog} , we keep the leading term (38) in the value of the quasi-particle annihilation operator just after the pulse, to obtain

$$\hat{D} \simeq - \sum_{\mathbf{k} \neq 0} (U_{\mathbf{k}} + V_{\mathbf{k}})^2 (\hat{A}_{\mathbf{k}}^\dagger \hat{B}_{\mathbf{k}} + \hat{B}_{\mathbf{k}}^\dagger \hat{A}_{\mathbf{k}}) \quad (46)$$

This scales with N as $N^{1/2}$ since each term has a zero mean. Intuitively, this scales with ϵ_{Bog} as $\epsilon_{\text{Bog}}^{1/2}$: $\hat{B}_{\mathbf{k}}$ is of order unity since it corresponds to vacuum field fluctuations in the initial empty state b , and $\hat{A}_{\mathbf{k}}$ is of order $\epsilon_{\text{Bog}}^{1/2}$ since it corresponds to the initial non-condensed field fluctuations in state a . We thus conclude that

$$\hat{D} \approx (N\epsilon_{\text{Bog}})^{1/2} \quad (47)$$

This is confirmed by the correlation functions of \hat{A} and \hat{B} given in the Appendix C, that allow an explicit calculation of $\langle \hat{D}^2 \rangle / N$, which is indeed $\approx \epsilon_{\text{Bog}}$, see Eqs.(61,62).

The same analysis is applied to the various operators appearing in the antihermitian part of (43), writing for simplicity $\hat{F} = \hat{F}_R + i\hat{F}_I$, where \hat{F}_R and \hat{F}_I are hermitian. It is found in the Appendix D that

$$\hat{\theta}_a - \hat{\theta}_b \approx \frac{1}{N^{1/2}} \quad (48)$$

$$\hat{F}_I \approx (N\epsilon_{\text{Bog}})^{1/2} \quad (49)$$

$$\hat{F}_R \approx N\epsilon_{\text{Bog}} \pm (N\epsilon_{\text{Bog}})^{1/2} \quad (50)$$

Contrarily to the first two operators, \hat{F}_R has a non-zero expectation value, and the writing of its estimate respectively corresponds to its mean value and its standard deviation. It turns out that the fluctuations of \hat{F}_R are negligible so that the operator can be replaced by its mean value. The weak value of the phase difference operator shows that its exponential in (43) can be expanded to first order, which substantially simplifies the calculations. The final result, up to zeroth order included in ϵ_{size} and up to first order included in ϵ_{Bog} , is

$$\langle \hat{S}_x \rangle = \frac{N}{2} \left(1 + 2 \frac{\langle \hat{F}_R \rangle}{N} \right) \quad (51)$$

$$\begin{aligned} \frac{\langle \hat{S}_y^2 \rangle}{N} &= \frac{\langle \hat{F}_I^2 \rangle}{N} + \langle (\hat{\theta}_a - \hat{\theta}_b)^2 \rangle \left(\frac{N}{4} + \langle \hat{F}_R \rangle \right) \\ &\quad - \frac{1}{2} \langle \{\hat{F}_I, \hat{\theta}_a - \hat{\theta}_b\} \rangle \end{aligned} \quad (52)$$

$$\begin{aligned} \frac{\langle \{\hat{S}_y, \hat{S}_z\} \rangle}{N} &= -\frac{1}{2N} \left(\frac{N}{2} + \langle \hat{F}_R \rangle \right) \\ &\quad \times \langle \{\hat{N}_a - \hat{N}_b, \hat{\theta}_a - \hat{\theta}_b\} \rangle \end{aligned} \quad (53)$$

Note that these expressions hold independently of the approximation performed in the phase difference operator (that neglects the oscillating terms).

C. Results of the expansion method for $\xi^2(t)$

To obtain an expression for ξ^2 in the double thermodynamic and Bogoliubov limit, it remains to explicitly evaluate (51,52,53) and to insert the result in (3,41). The required operators have their expression given in useful form in the Appendix D, and by (35,37,46) for the phase difference operator.

We have first evaluated (51,52,53) at time $t = 0^+$, and we have checked that one recovers the exact relations $\langle \hat{S}_x \rangle(0^+) = N/2$, $\langle \hat{S}_y^2 \rangle(0^+) = N/4$ and $\langle \{\hat{S}_y, \hat{S}_z\} \rangle(0^+) = 0$. At finite time, squaring (35), one realizes that the crossed term, linear in time, has a zero expectation value since

$$\langle (\hat{\theta}_a - \hat{\theta}_b)(0^+) (\hat{N}_a - \hat{N}_b) \rangle = \langle (\hat{\theta}_a - \hat{\theta}_b)(0^+) \hat{D} \rangle = 0 \quad (54)$$

This is due to the fact that the phase difference operator at $t = 0^+$ is proportional to the antihermitian part $i\hat{y}$ of $e^{-i\hat{\theta}_a^{(0)}\hat{b}_0^{(0)}}$, whereas $\hat{N}_a - \hat{N}_b$ only involves the hermitian

part \hat{x} and $\hat{\mathcal{D}}$ does not depend on that operator. As a consequence, the spreading of the relative phase is purely ballistic within our Bogoliubov approximation, that it ignores the interactions among the quasi-particles

$$\langle(\hat{\theta}_a - \hat{\theta}_b)^2\rangle = \langle(\hat{\theta}_a - \hat{\theta}_b)^2\rangle(0^+) + (\chi t)^2 \langle(\hat{N}_a - \hat{N}_b + \hat{\mathcal{D}})^2\rangle \quad (55)$$

(the inclusion of these interactions within a quantum kinetic framework introduces a diffusive component in the phase spreading [18]). Another simplification takes place, for similar reasons,

$$\langle\hat{F}_I(\hat{N}_a - \hat{N}_b + \hat{\mathcal{D}})\rangle \in i\mathbb{R} \quad (56)$$

so the last term of (52) reduces to its $t = 0^+$ value. Using (42), and the fact that $\langle\hat{F}_R\rangle$, $\langle\hat{\mathcal{D}}^2\rangle$ and $\langle\{\hat{S}_z, \hat{\mathcal{D}}\}\rangle$ are all $\approx N\epsilon_{\text{Bog}}$, and neglecting contributions in ϵ_{Bog}^2 , we finally obtain

$$\frac{\langle\hat{S}_y^2\rangle - \langle\hat{S}_z^2\rangle}{N} = \tau^2 \left(1 + \frac{\langle\hat{\mathcal{D}}^2\rangle}{N}\right) + \frac{\langle\hat{F}_R\rangle}{N} \quad (57)$$

$$\frac{\langle\{\hat{S}_y, \hat{S}_z\}\rangle}{N} = \tau \quad (58)$$

where we have introduced a dimensionless “time”

$$\tau(t) \equiv \frac{\rho g t}{2\hbar} \left(1 + \frac{2\langle\hat{F}_R(t)\rangle + \langle\{\hat{S}_z, \hat{\mathcal{D}}\}\rangle}{N}\right) \quad (59)$$

that is slightly renormalized by a time dependent contribution of order ϵ_{Bog} . The expectation values appearing in (59) are given in the Appendix D, they are respectively uniformly bounded in time and time independent. Note that the long-time behaviors of (57,58) were expected: As the squeezing dynamic occurs, \hat{S}_y indeed grows quadratically in time while \hat{S}_z stays constant.

Expanding (41) up to order one included in ϵ_{Bog} at any fixed τ finally gives the squeezing parameter as a function of time in the thermodynamic limit (in particular for $\tau \ll N^{1/2}$):

$$\xi^2(t) \simeq \frac{1 - 4\frac{\langle\hat{F}_R\rangle}{N}}{(\tau + \sqrt{1 + \tau^2})^2} + \frac{2\left(\frac{\langle\hat{\mathcal{D}}^2\rangle}{N}\tau^2 + \frac{\langle\hat{F}_R\rangle}{N}\right)}{(\tau + \sqrt{1 + \tau^2})\sqrt{1 + \tau^2}} \quad (60)$$

As we show in Fig.4, the squeezing parameter $\xi^2(t)$ decreases in time essentially as in the two-mode model [this is the first term in the right hand side of (60) without the $\langle\hat{F}_R\rangle/N$ term, see e.g. equation (52) in [11]] until a renormalized time $\tau \approx 1/\sqrt{\epsilon_{\text{Bog}}} \gg 1$ is reached, when the multimode effects [the second term] start limiting the squeezing. At such times, the contribution of $\langle\hat{\mathcal{D}}^2\rangle/N$ dominates over the one of $\langle\hat{F}_R\rangle/N$ by a factor $\approx 1/\epsilon_{\text{Bog}}^2$, which shows that $\langle\hat{\mathcal{D}}^2\rangle/N$ constitutes the real actor in the process of squeezing limitation.

D. Minimal squeezing and best squeezing time

From the central result (60) of the previous subsection, it appears that the minimal squeezing ξ_{min}^2 is reached in

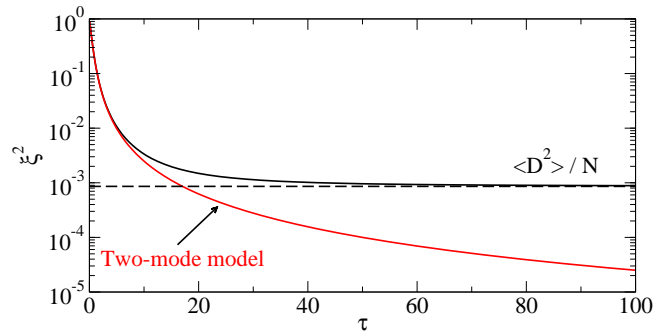


FIG. 4: (Color online) Black solid line: Squeezing parameter in the thermodynamic and weakly interacting limit (60) as a function of the renormalized time τ (59). Parameters: $k_B T/\rho g = 1$ and $\sqrt{\rho a^3} = 10^{-3}$. Black dashed line: asymptotic value (61). Red solid line: two-mode model prediction.

the thermodynamic and Bogoliubov limits at “infinite” time and it is given by

$$\xi_{\text{min}}^2 = \frac{\langle\hat{\mathcal{D}}^2\rangle}{N} \quad (61)$$

As explained above (47), an explicit calculation gives:

$$\xi_{\text{min}}^2 = \int \frac{d^3 k}{(2\pi)^3} \frac{s_k^4}{2\rho} \left[\left(n_k^{(0)} + \frac{1}{2}\right) \left(\frac{(s_k^{(0)})^2}{s_k^4} + \frac{s_k^4}{(s_k^{(0)})^2}\right) - 1 \right] \quad (62)$$

where we have introduced the mean occupation numbers $n_k^{(0)} = 1/[\exp(\beta\epsilon_k^{(0)}) - 1]$ of the Bogoliubov quasi-particles in the initial ($t = 0^-$) thermal equilibrium gas in internal state a . The prediction of (62) is shown as a dashed line in Fig.3 and as a full line in Fig.5. In Fig.5 we show that the minimal squeezing parameter given by (62) is always lower than the non condensed fraction $\langle N_{\text{nc}}\rangle/N$ where $\langle N_{\text{nc}}\rangle \equiv \langle\hat{N}_{a\pm}^{(0)}\rangle$ is the mean number of non condensed atoms in component a before the pulse:

$$\langle N_{\text{nc}}\rangle = \sum_{\mathbf{k} \neq \mathbf{0}} \left[\left(U_{\mathbf{k}}^{(0)}\right)^2 + \left(V_{\mathbf{k}}^{(0)}\right)^2 \right] n_{\mathbf{k}}^{(0)} + \left(V_{\mathbf{k}}^{(0)}\right)^2 \quad (63)$$

Asymptotically, for $k_B T \gg \rho g$ (but always $T \ll T_c$) the minimal squeezing parameter ξ_{min}^2 reaches the non condensed fraction. In the opposite limit, for $k_B T/\rho g \rightarrow 0$, the squeezing tends to a constant value.

$$\frac{\xi_{\text{min}}^{2(T=0)}}{\sqrt{\rho a^3}} = \sqrt{\frac{8}{\pi}} \left[\frac{19}{6} \sqrt{2} - \frac{3}{2} \ln(\sqrt{2} + 1) - \pi \right] \simeq 0.02344 \quad (64)$$

Although non zero, $\xi_{\text{min}}^{2(T=0)}$ is very small for practical purposes. Indeed $\rho a^3 < 10^{-6}$ in present squeezing experiments so that (64) predicts $\xi_{\text{min}}^{2(T=0)} \lesssim 2 \times 10^{-5}$.

The fact that the minimal squeezing is obtained at infinite time is a limitation of our Bogoliubov approach, that neglects the interactions between the quasi-particles

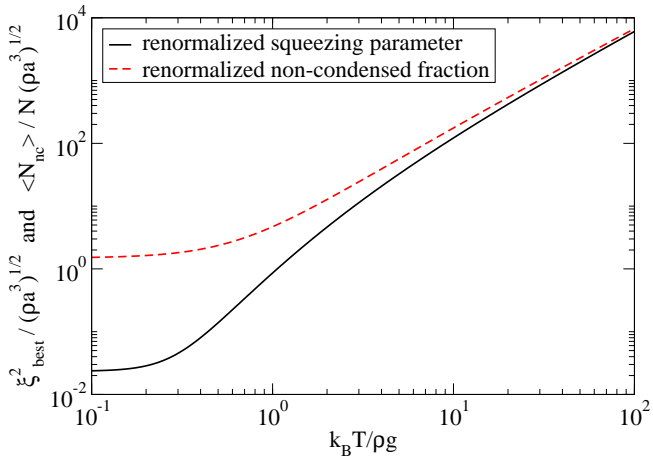


FIG. 5: (Color online). Minimal squeezing (black solid line) ξ_{\min}^2 and non condensed fraction (red dashed line) $\langle N_{\text{nc}} \rangle / N$, both divided by $\sqrt{\rho a^3}$, as a function of $k_B T / \rho g$.

and effectively assumes that the corresponding collision time is diverging, see discussion below. However, since the numerical squeezing curve $\xi^2(t)$ is quite flat around its minimum (see Fig.8), it suffices in practice to determine a “close to best” squeezing time t_η defined as $\xi^2(t_\eta) = (1 + \eta)\xi_{\min}^2$, where $\eta > 0$. Then, according to (60) expanded for large τ up to order τ^{-2} included, t_η is finite and given for $\eta \ll 1$ by

$$\frac{\rho g}{\hbar} t_\eta \simeq \frac{1}{\sqrt{\eta \xi_{\min}^2}} \quad (65)$$

The “close to best” squeezing time t_η (65) for $\eta = 0.2$ is shown in Fig.6 as a full line and compared to simulations (filled symbols).

An important issue is that of *thermalization* that brings the system back to equilibrium after the pulse. Thermalization is neglected in the Bogoliubov theory and in our analytics but it is included in the classical field simulations. It is thus possible to reach $\xi^2 = (1 + \eta)\xi_{\min}^2$ only if t_η given by (65) is shorter than the thermalization time:

$$t_\eta < t_{\text{therm}} \quad (66)$$

We show the thermalization times, that we extract from the classical simulations as explained in [9], as empty symbols in Fig.6. For the points we considered they are indeed longer than the close to best squeezing times and the condition (66) is satisfied. We can also estimate t_{therm} from Landau-Beliaev damping rates of Bogoliubov modes [17, 35]. The damping rate of the mode \mathbf{q} is

$$\Gamma_q = \frac{g}{2\pi^2 \hbar \xi^3} (\check{\Gamma}_q^L + \check{\Gamma}_q^B) \quad (67)$$

where the healing length ξ is defined by $\rho g = \hbar^2 / (2m\xi^2)$ and the rescaled Landau and Beliaev damping rates $\check{\Gamma}_q^L$ and $\check{\Gamma}_q^B$ are dimensionless functions of $k_B T / \rho g$ only, given

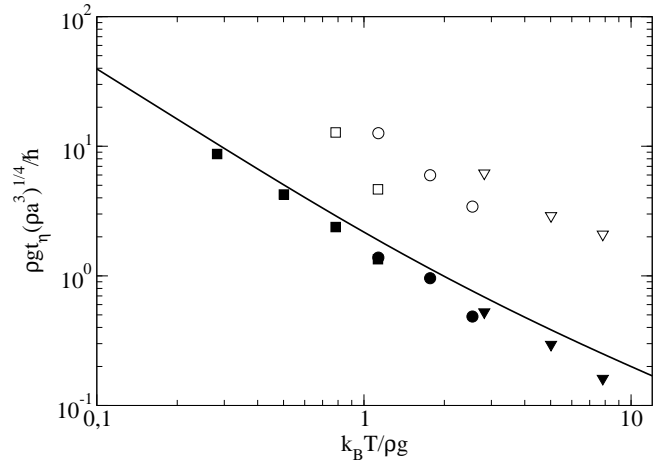


FIG. 6: Universal scaling of the “close to best” squeezing time t_η with $\eta = 0.2$. Filled symbols: classical field simulations with $\sqrt{\rho a^3} = 1.32 \times 10^{-2}$ (squares), 1.94×10^{-3} (disks) and $\sqrt{\rho a^3} = 4.317 \times 10^{-4}$ (triangles). Solid line: analytical result (65) using (21). The empty symbols (squares, circles and triangles) show the thermalization times t_{therm} extracted from the simulations as explained in [9]. Parameters are as in Fig.3.

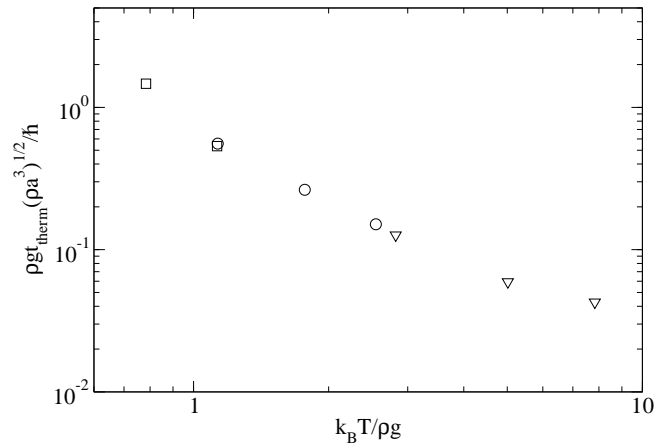


FIG. 7: Scaling with $(\rho a^3)^{-1/2}$ of the thermalization times extracted from the classical field simulations. $\sqrt{\rho a^3} = 1.32 \times 10^{-2}$ (squares), 1.94×10^{-3} (circles) and $\sqrt{\rho a^3} = 4.317 \times 10^{-4}$ (triangles).

e.g. in equations (A7) and (A13) of [17]. Concentrating of the pre-factor in (67), for fixed $k_B T / \rho g$, this gives

$$\frac{\rho g t_{\text{therm}}}{\hbar} \simeq \frac{\rho g}{\hbar \Gamma_q} = \sqrt{\frac{\pi}{128}} (\check{\Gamma}_q^L + \check{\Gamma}_q^B)^{-1} \frac{1}{\sqrt{\rho a^3}} \quad (68)$$

The scaling with $(\rho a^3)^{-1/2}$ of the thermalization time is shown in Fig.7. On the other hand, the close to best squeezing time t_η scales as

$$\frac{\rho g t_\eta}{\hbar} \propto \frac{1}{(\rho a^3)^{1/4}} \quad \text{so that} \quad \frac{t_\eta}{t_{\text{therm}}} \propto (\rho a^3)^{1/4} \quad (69)$$

and (66) is satisfied in the weakly interacting limit.

V. PHYSICAL INTERPRETATION

A. Limit to the squeezing

In the spin squeezing scheme with condensates that we consider, the useful quantum correlations are built through mean field interactions that introduces a phase shift for each atom that depends on the collective variable $N_a - N_b$. In the collective spin picture, we can say that in a given realization of the experiment, the component \hat{S}_y becomes an enlarged copy of \hat{S}_z so that correlations build up in the S_y - S_z plane, orthogonally to mean spin. To explain this fact in a simple reasoning, we can identify \hat{S}_y with the condensate relative phase: $\hat{S}_y \simeq \frac{N}{2}(\hat{\theta}_a - \hat{\theta}_b)$ and look at equation (35) that we rewrite here replacing χ by its expression $\chi = g/(\hbar V)$:

$$\hat{\theta}_a - \hat{\theta}_b = (\hat{\theta}_a - \hat{\theta}_b)(0^+) - \frac{\rho g t}{\hbar N} \left[\hat{N}_a - \hat{N}_b + \hat{\mathcal{D}} \right] \quad (70)$$

Initially, at $t = 0$, the phase difference $(\hat{\theta}_a - \hat{\theta}_b)(0^+)$ is of order $1/\sqrt{N}$ and $N_a - N_b$ is of order \sqrt{N} . As soon as $\rho g t/\hbar \gg 1$, the time dependent term in (70) dominates over the initial condition. In the absence of the multimode contribution to the phase difference (i.e. for $\hat{\mathcal{D}} = 0$), $\hat{\theta}_a - \hat{\theta}_b$ and thus \hat{S}_y become an enlarged copy of $\hat{S}_z = (\hat{N}_a - \hat{N}_b)/2$. This is the scenario in the two-mode theory. Correlations between \hat{S}_y and \hat{S}_z becomes perfect in the long time limit. In this case there is no limit to the squeezing and $\xi_{\min}^2 \rightarrow 0$ when $N \rightarrow \infty$. On the other hand, in the presence of $\hat{\mathcal{D}}$ this is not possible. Looking at squeezing in the long time limit where where $|\hat{S}_y| \gg |\hat{S}_z|$ and keeping only the leading (0^{th}) order in $1/t$ in equation (60), we can write

$$\xi^2(t) \simeq \frac{\langle \hat{S}_y^2 \rangle \langle \hat{S}_z^2 \rangle - \langle \{ \hat{S}_y, \hat{S}_z \} / 2 \rangle^2}{\langle \hat{S}_y^2 \rangle \langle \hat{S}_z^2 \rangle} \simeq \frac{\langle \hat{\mathcal{D}}^2 \rangle}{N} = \xi_{\min}^2 \quad (71)$$

The only contribution left in ξ_{\min}^2 is the variance of $\hat{\mathcal{D}}$ that is the part of $\theta_a - \theta_b$ that is not proportional to $N_a - N_b$. But what is the physical origin of $\hat{\mathcal{D}}$, given by (36)? It comes from the fact that the mean field interaction for a condensed atom with and another condensed atom or with an atom in an excited mode is not the same. This is particularly clear in the Hartree-Fock limit where $V_k \rightarrow 0$ and $U_k \rightarrow 1$. In this case $\hat{\mathcal{D}}$ reduces to $\hat{N}_{a\perp} - \hat{N}_{b\perp}$ that is the non-condensed atom number difference. In this limit we have

$$\left(\hat{\theta}_a - \hat{\theta}_b \right)_{\text{HF}} \simeq -\frac{\rho g t}{\hbar N} \left[\hat{N}_{a0} - \hat{N}_{b0} + 2 \left(\hat{N}_{a\perp} - \hat{N}_{b\perp} \right) \right] \quad (72)$$

the factor 2 is the Hartree-Fock factor that doubles the effective strength of the condensate-non condensate interaction with respect to the condensate-condensate interaction.

B. Squeezing of the condensate mode

In Fig.8 (a) and (b), for two temperatures: $k_B T \gg \rho g$ and $k_B T < \rho g$, we compare the squeezing of the total field ξ^2 , that we have been considering so far, with the one of the condensate mode ξ_0^2 , constructed with a spin operator involving the condensate mode only: $\hat{S}_{0x} + i\hat{S}_{0y} = \hat{a}_0^\dagger \hat{b}_0$ and $\hat{S}_{0z} = \hat{N}_{a0} - \hat{N}_{b0}$:

$$\xi_0^2 = \frac{N_{a0} \Delta S_{0\perp, \min}^2}{|\langle \mathbf{S}_0 \rangle|^2}, \quad (73)$$

This is the squeezing that would be obtained by “selecting” only the condensed particles for the squeezing measurement. Clearly $\xi^2 \ll \xi_0^2$ in both graphs. Particularly striking is the case in Fig.8(b) where $\xi_{0\min}^2/\xi_{\min}^2 \simeq 60$ while the non condensed fraction is only $\langle N_{\text{nc}} \rangle/N = 0.02$. We explain here why this is the case. In order to have condensate squeezing we need correlations between \hat{S}_{0y} , that is still proportional to $\hat{\theta}_a - \hat{\theta}_b$, and \hat{S}_{0z} . In the Hartree-fock limit, Fig.8 (a), one thus expects $\xi_{0\min}^2 = 4\xi_{\min}^2 \simeq 4\langle N_{\text{nc}} \rangle/N$ where $\langle N_{\text{nc}} \rangle = \text{Var}(N_{a\perp} - N_{b\perp})$ is the non condensed fraction in component a before the pulse. In the Bogoliubov limit, $\hat{\mathcal{D}} \neq \hat{N}_{a\perp} - \hat{N}_{b\perp}$. Then for the squeezing of the condensate we have

$$\xi_{0\min}^2 = \frac{\langle N_{\text{nc}} \rangle + \langle \hat{\mathcal{D}}^2 \rangle + \langle \{ \hat{\mathcal{D}}, (\hat{N}_{a\perp} - \hat{N}_{b\perp}) \} \rangle}{N} \quad (74)$$

In practice at low temperature $k_B T \ll \rho g$ one can have $\langle \hat{\mathcal{D}}^2 \rangle \ll \langle N_{\text{nc}} \rangle$ and $\xi_{0\min}^2$ can exceed ξ_{\min}^2 by more than one order of magnitude although the non-condensed fraction is very small. This is illustrated in Fig.8 (b). Besides the classical field simulations, in Fig.8 (a) and (b) we also show as dashed curves results obtained in the Bogoliubov approximation as follows. Before the pulse, we start with a thermalized field sampling (12). After the pulse, we evolve the condensate phase with the classical equivalent of (34), also performing in that equation the approximation of neglecting the oscillating terms, and the Bogoliubov amplitudes with (32). The condensate atom numbers are obtained by the classical equivalent of (33). Note that, for an accurate the condensate squeezing, it is important to keep the oscillating terms in $N_{a\perp}(t)$ and $N_{b\perp}(t)$.

VI. CONCLUSION

We have shown that, in a multimode theory, the spin squeezing that can be obtained dynamically using interactions in condensates is finite in the thermodynamic limit. This is contrary to the results of the currently used two-mode theory that predicts an infinite metrology gain for $N \rightarrow \infty$. Using a convenient reformulation of the Bogoliubov theory, we could calculate the temperature and interactions dependent limit of the spin squeezing parameter analytically for a spatially homogeneous system. We

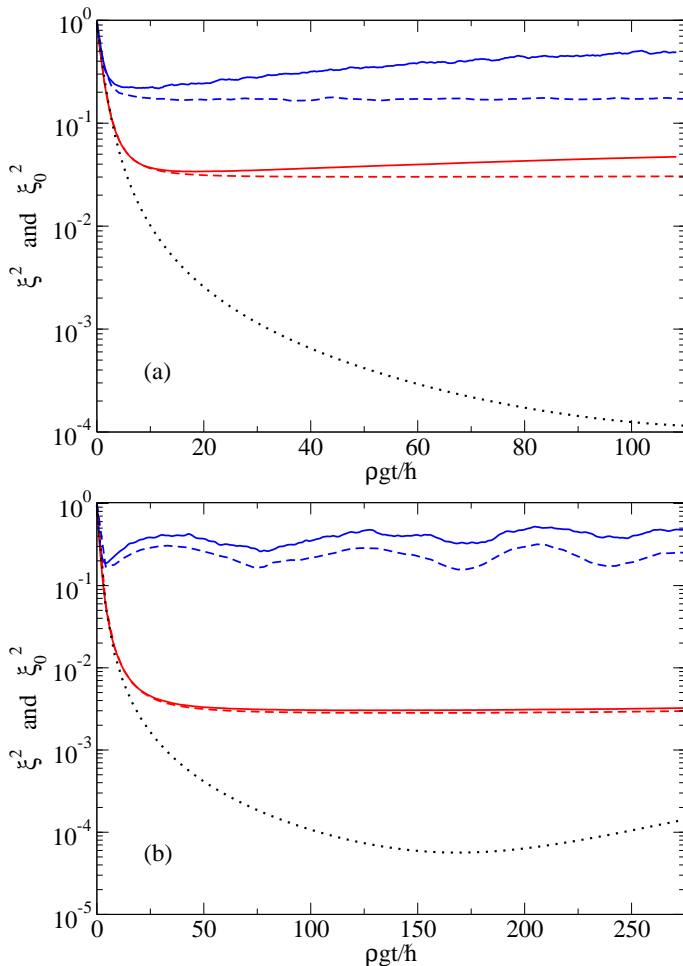


FIG. 8: (Color online). Condensate squeezing ξ_0^2 (blue upper curves) and squeezing of the total field ξ^2 (red middle curves) as a function of time. Full lines: classical field simulation, Dashed lines: Bogoliubov (see text), The two-mode result (black lowest dotted lines) is shown for comparison. Upper graph: $k_B T / \rho g = 7.83$, $\langle N_{nc} \rangle / N = 0.05$, $N = 983040$, $\rho g = 693.6 \hbar^2 / m V^{2/3}$, $\sqrt{\rho a^3} = 4.17 \times 10^{-4}$. Lower graph: $k_B T / \rho g = 0.5$, $\langle N_{nc} \rangle / N = 0.02$, $N = 2733750$, $\rho g = 13715.9 \hbar^2 / m V^{2/3}$, $\sqrt{\rho a^3} = 1.32 \times 10^{-2}$.

performed non perturbative classical field simulations to test our analytical results including interactions among Bogoliubov modes and thermalization that are neglected in the perturbative treatment.

At temperatures $k_B T \ll \rho g$ the limit that we find for the squeezing parameter optimized over time, ξ_{\min}^2 , is very small and in particular much smaller than what is currently measured in present experiments. Nevertheless it represent the fundamental limit of this squeezing scheme and we hope that the temperature dependent limitation to spin squeezing will be soon within reach of experiments. We explained that the physical origin to this limit of the squeezing lies in the difference of mean field interactions between condensate-condensate and condensate-non condensed atoms.

Acknowledgments

A.S. acknowledges useful discussions with J. Reichel and J. Estève. E.W. acknowledges support from CNRS and Polish GRF: N N202 128539.

Appendix A: Some useful relations

Here we collect useful commutation relations and recall the expression of the Bogoliubov quasi-particle annihilation operators $\hat{c}_{\sigma \mathbf{k}}$ after the mixing pulse in terms of the atomic annihilation and creation operators.

Commutation relations: In our lattice model, the field operators obey discrete bosonic commutation relations:

$$[\hat{\psi}_{\sigma}(\mathbf{r}), \hat{\psi}_{\sigma'}^{\dagger}(\mathbf{r}')] = \frac{\delta_{\mathbf{r}, \mathbf{r}'} \delta_{\sigma, \sigma'}}{dV} \quad \forall \sigma, \sigma' = a, b \quad (\text{A1})$$

The hermitian condensate number and phase operators obey, for $\sigma, \sigma' = a, b$:

$$[\hat{N}_{\sigma \mathbf{0}}, \hat{\theta}_{\sigma'}] = i \delta_{\sigma, \sigma'} \quad (\text{A2})$$

The fields of the non-condensed modes, orthogonal to the condensate wavefunction, obey

$$[\hat{\psi}_{\sigma \perp}(\mathbf{r}), \hat{\psi}_{\sigma' \perp}^{\dagger}(\mathbf{r}')] = \frac{\delta_{\sigma, \sigma'} \delta_{\mathbf{r}, \mathbf{r}'}}{dV} - \frac{\delta_{\sigma, \sigma'}}{V} \quad (\text{A3})$$

The non-condensed fields do not commute with the the total atom number but they commute with all the condensate operators:

$$[\hat{N}_{\sigma \mathbf{0}}, \hat{\psi}_{\sigma' \perp}(\mathbf{r})] = [\hat{\theta}_{\sigma}, \hat{\psi}_{\sigma' \perp}(\mathbf{r})] = 0 \quad (\text{A4})$$

The number-conserving operators $\hat{\Lambda}_{\sigma}$ obey the same commutation relations (A3) as the non-condensed fields, e. g.

$$[\hat{\Lambda}_{\sigma}(\mathbf{r}), \hat{\Lambda}_{\sigma'}^{\dagger}(\mathbf{r}')] = \frac{\delta_{\mathbf{r}, \mathbf{r}'}}{dV} - \frac{1}{V} \quad \forall \sigma = a, b \quad (\text{A5})$$

but, contrarily to them, they commute with the total atom number operators in each component:

$$[\hat{\Lambda}_{\sigma}(\mathbf{r}), \hat{N}_{\sigma'}] = 0 \quad \forall \sigma, \sigma' = a, b \quad (\text{A6})$$

Their commutation relations with the condensate operators are, for $\sigma, \sigma' = a, b$:

$$[\hat{\Lambda}_{\sigma}(\mathbf{r}), \hat{\theta}_{\sigma'}] = 0, \quad [\hat{\Lambda}_{\sigma}(\mathbf{r}), \hat{N}_{\sigma' \mathbf{0}}] = -\hat{\Lambda}_{\sigma}(\mathbf{r}) \delta_{\sigma, \sigma'} \quad (\text{A7})$$

Finally, from the relation $e^{-i\hat{\theta}_a} f(\hat{N}_{a\mathbf{0}}) e^{i\hat{\theta}_a} = f(\hat{N}_{a\mathbf{0}} - 1)$ resulting from (A2), for a generic function f , we have in the large N , and thus large $\hat{N}_{a\mathbf{0}}$ limit:

$$\left[\sqrt{\hat{N}_{a\mathbf{0}}}, e^{i\hat{\theta}_a} \right] = -e^{i\hat{\theta}_a} \frac{1}{2\sqrt{\hat{N}_{a\mathbf{0}}}} + O\left(\frac{1}{N^{3/2}}\right) \quad (\text{A8})$$

Bogoliubov transformations: By projecting (29) over the plane waves, we obtain after the pulse ($t > 0$):

$$\hat{a}_{\mathbf{k}} = e^{i\hat{\theta}_a} \left(\hat{c}_{a\mathbf{k}} U_k + \hat{c}_{a-\mathbf{k}}^\dagger V_k \right) \quad (\text{A9})$$

$$\hat{b}_{\mathbf{k}} = e^{i\hat{\theta}_b} \left(\hat{c}_{b\mathbf{k}} U_k + \hat{c}_{b-\mathbf{k}}^\dagger V_k \right) \quad (\text{A10})$$

where $\hat{a}_{\mathbf{k}}$ and $\hat{b}_{\mathbf{k}}$ annihilate an atom with internal state a, b and wave vector \mathbf{k} . The inverse relations are useful:

$$\hat{c}_{a\mathbf{k}} = e^{-i\hat{\theta}_a} \hat{a}_{\mathbf{k}} U_k - \hat{a}_{-\mathbf{k}}^\dagger e^{i\hat{\theta}_a} V_k \quad (\text{A11})$$

$$\hat{c}_{b\mathbf{k}} = e^{-i\hat{\theta}_b} \hat{b}_{\mathbf{k}} U_k - \hat{b}_{-\mathbf{k}}^\dagger e^{i\hat{\theta}_b} V_k \quad (\text{A12})$$

with U_k, V_k given by (30).

Appendix B: After-pulse values of the condensate phases and quasi-particle annihilation operators

To determine the condensate phase operator for the internal state σ at time $t = 0^+$ in terms of operators at $t = 0^-$, we use the fact resulting from (9,10) that $a_{\mathbf{0}}(0^+) = [a_{\mathbf{0}}^{(0)} - b_{\mathbf{0}}^{(0)}]/\sqrt{2}$ and $b_{\mathbf{0}}(0^+) = [a_{\mathbf{0}}^{(0)} + b_{\mathbf{0}}^{(0)}]/\sqrt{2}$. Then the definition (23) leads to

$$e^{i\hat{\theta}_\sigma(0^+)} = e^{i\hat{\theta}_\sigma^{(0)}} \left(\sqrt{\hat{N}_{a\mathbf{0}}^{(0)}} \mp \tilde{b}_{\mathbf{0}}^{(0)} \right) \left| \sqrt{\hat{N}_{a\mathbf{0}}^{(0)}} \mp \tilde{b}_{\mathbf{0}}^{(0)} \right|^{-1} \quad (\text{B1})$$

where the upper sign ($-$) is for $\sigma = a$ and the lower sign ($+$) for $\sigma = b$, the modulus operator of an operator \hat{X} is

$$|\hat{X}| \equiv \left(\hat{X}^\dagger \hat{X} \right)^{1/2} \quad (\text{B2})$$

and we have introduced the number conserving operator $\tilde{b}_{\mathbf{0}}^{(0)} = e^{-i\hat{\theta}_a^{(0)}} \hat{b}_{\mathbf{0}}^{(0)}$. By expanding in the large $\hat{N}_{a\mathbf{0}}^{(0)}$ limit, we obtain :

$$\hat{\theta}_\sigma(0^+) - \hat{\theta}_\sigma^{(0)} = \text{Herm} \left[\mp \hat{y} \left(\hat{N}_{a\mathbf{0}}^{(0)} \right)^{-1/2} - \frac{1}{2} \{ \hat{x}, \hat{y} \} \left(\hat{N}_{a\mathbf{0}}^{(0)} \right)^{-1} + O \left(\frac{1}{N^{3/2}} \right) \right] \quad (\text{B3})$$

We have introduced the decomposition $\tilde{b}_{\mathbf{0}}^{(0)} = \hat{x} + i\hat{y}$, where \hat{x} and \hat{y} are hermitian operators, the usual notation $\{, \}$ for the anticommutator and the notation $\text{Herm} \hat{X} = (\hat{X} + \hat{X}^\dagger)/2$ for the hermitian part of an operator \hat{X} . This leads to (37).

To determine the quasi-particle annihilation operators $\hat{c}_{\sigma\mathbf{k}}$ at time $t = 0^+$ in terms of operators at time $t = 0^-$, we use the relations (A11,A12) to express them in terms of the atomic creation and annihilation operators at time $t = 0^+$, that are in turn expressed in terms of their values at 0^- thanks to (9,10). One also needs the expansion $\exp[i\hat{\theta}_\sigma(0^+)] = \exp[i\hat{\theta}_\sigma^{(0)}][1 + i(\hat{\theta}_\sigma(0^+) - \hat{\theta}_\sigma^{(0)}) + O(1/N)]$ deduced from (B3) and the Hausdorff formula. With the

short-hand notations $\tilde{a}_{\mathbf{k}}^{(0)} = \exp(-i\hat{\theta}_a^{(0)})\hat{a}_{\mathbf{k}}^{(0)}$ and $\tilde{b}_{\mathbf{k}}^{(0)} = \exp(-i\hat{\theta}_a^{(0)})\hat{b}_{\mathbf{k}}^{(0)}$:

$$\hat{c}_{\sigma\mathbf{k}}(0^+) = \frac{U_k \tilde{a}_{\mathbf{k}}^{(0)} - V_k \tilde{a}_{-\mathbf{k}}^{(0)\dagger}}{\sqrt{2}} \mp \frac{U_k \tilde{b}_{\mathbf{k}}^{(0)} - V_k \tilde{b}_{-\mathbf{k}}^{(0)\dagger}}{\sqrt{2}} - i \left[\hat{\theta}_\sigma(0^+) - \hat{\theta}_\sigma^{(0)} \right] \left[\frac{U_k \tilde{a}_{\mathbf{k}}^{(0)} + V_k \tilde{a}_{-\mathbf{k}}^{(0)\dagger}}{\sqrt{2}} \mp \frac{U_k \tilde{b}_{\mathbf{k}}^{(0)} + V_k \tilde{b}_{-\mathbf{k}}^{(0)\dagger}}{\sqrt{2}} \right] + O \left(\frac{1}{N} \right) \quad (\text{B4})$$

where the upper, $-$ sign is for $\sigma = a$ and the lower, $+$ sign if for $\sigma = b$. One then introduces the operators

$$\hat{A}_{\mathbf{k}} = U_k \tilde{a}_{\mathbf{k}}^{(0)} - V_k \tilde{a}_{-\mathbf{k}}^{(0)\dagger} \quad \text{and} \quad \hat{B}_{\mathbf{k}} = U_k \tilde{b}_{\mathbf{k}}^{(0)} - V_k \tilde{b}_{-\mathbf{k}}^{(0)\dagger} \quad (\text{B5})$$

This directly gives (40). Expressing $\tilde{a}_{\mathbf{k}}^{(0)}$ and $\tilde{a}_{-\mathbf{k}}^{(0)\dagger}$ in terms of the pre-pulse quasi-particle annihilation and creation operators thanks to the $t = 0^-$ equivalent of (A9), gives (39). Restricting the accuracy of (B4) to $O(1)$ included, gives (38).

Appendix C: Correlations of $\hat{A}_{\mathbf{k}}$ and $\hat{B}_{\mathbf{k}}$

Some useful properties of the operators defined in (39,40) [or equivalently in (B5)] are given here. The commutation relations of these operators are bosonic. This means that the only non-zero commutators (considered among all possible values of \mathbf{k}) are

$$\left[\hat{A}_{\mathbf{k}}, \hat{A}_{\mathbf{k}}^\dagger \right] = \left[\hat{B}_{\mathbf{k}}, \hat{B}_{\mathbf{k}}^\dagger \right] = 1 \quad (\text{C1})$$

To calculate averages of products of \hat{A} and \hat{B} operators (here at equal times) one can use the Wick theorem as the initial density operator for $\{c_{a\mathbf{k}}^{(0)}\}$ and $\{b_{\mathbf{k}}^{(0)}\}$ is a Gaussian. All the non-zero correlations involving the $\hat{A}_{\mathbf{k}}$ can be deduced from

$$\langle \hat{A}_{\mathbf{k}}^\dagger \hat{A}_{\mathbf{k}} \rangle = \frac{1}{2} \left(n_{\mathbf{k}}^{(0)} + \frac{1}{2} \right) \left[\frac{s_k^{(0)2}}{s_k^2} + \frac{s_k^2}{s_k^{(0)2}} \right] - \frac{1}{2} \quad (\text{C2})$$

$$\langle \hat{A}_{\mathbf{k}} \hat{A}_{-\mathbf{k}} \rangle = \frac{1}{2} \left(n_{\mathbf{k}}^{(0)} + \frac{1}{2} \right) \left[\frac{s_k^{(0)2}}{s_k^2} - \frac{s_k^2}{s_k^{(0)2}} \right] \quad (\text{C3})$$

with $s_k^{(0)}$ and s_k defined by (28,30). All the non-zero correlations involving the $\hat{B}_{\mathbf{k}}$ can be deduced from

$$\langle \hat{B}_{\mathbf{k}}^\dagger \hat{B}_{\mathbf{k}} \rangle = V_k^2 = \frac{1}{4} \left(s_k^2 + \frac{1}{s_k^2} \right) - \frac{1}{2} \quad (\text{C4})$$

$$\langle \hat{B}_{\mathbf{k}} \hat{B}_{-\mathbf{k}} \rangle = -U_k V_k = -\frac{1}{4} \left(s_k^2 - \frac{1}{s_k^2} \right) \quad (\text{C5})$$

All the crossed second moments, for example of the form $\langle \hat{A} \hat{B} \rangle$ or $\langle \hat{A}^\dagger \hat{B} \rangle$, are zero.

Appendix D: Double expansion of some operators

As explained in the main text, to have a vanishing error on the squeezing parameter ξ^2 in the thermodynamic limit, it suffices to determine the operators \hat{S}_y and \hat{S}_z up to $\approx N^{1/2}$ included.

Case of \hat{S}_z : The operator $\hat{S}_z = (\hat{N}_a - \hat{N}_b)/2$ is a constant of motion, it can be evaluated at $t = 0^+$, and related with (9,10) to the fields at $t = 0^-$. Then one uses the modulus-phase representation for the condensate operator in a and one introduces the number-conserving fields $\hat{\Lambda}_a^{(0)}$ and $e^{-i\hat{\theta}_a^{(0)}}\psi_{b\perp}^{(0)}$ for the non-condensed modes, whose Fourier components can be expressed in terms of the operators $\hat{A}_{\mathbf{k}}$ and $\hat{B}_{\mathbf{k}}$ through (B5). The only approximation is then to neglect the commutator of \hat{y} with $(\hat{N}_{a0}^{(0)})^{1/2}$, which is $O(1/N^{3/2})$, to obtain

$$\hat{N}_a - \hat{N}_b \simeq - \left\{ \hat{x}, \sqrt{\hat{N}_{a0}^{(0)}} \right\} - \sum_{\mathbf{k} \neq 0} [(U_{\mathbf{k}}^2 + V_{\mathbf{k}}^2) \times (\hat{A}_{\mathbf{k}}^\dagger \hat{B}_{\mathbf{k}} + \hat{A}_{\mathbf{k}} \hat{B}_{\mathbf{k}}^\dagger) + 2U_{\mathbf{k}}V_{\mathbf{k}}(\hat{A}_{\mathbf{k}}^\dagger \hat{B}_{-\mathbf{k}}^\dagger + \hat{A}_{\mathbf{k}} \hat{B}_{-\mathbf{k}})] \quad (\text{D1})$$

We recall than \hat{x} and \hat{y} are defined below (B3). The operator \hat{S}_z has a zero expectation value, and a variance exactly equal to $N/4$, as already found by a more direct method in (42), so we reach the estimate

$$\hat{S}_z \approx N^{1/2} \quad (\text{D2})$$

With more lengthy calculations, we now deduce \hat{S}_y from the antihermitian part of \hat{S}_+ written in the form (43) and we then obtain \hat{S}_y^2 and $\{\hat{S}_y, \hat{S}_z\}$.

The phase difference: We first evaluate the scaling of the phase difference $\hat{\theta}_a - \hat{\theta}_b$ in the thermodynamic limit from the writing (35). The contribution of the phase difference at time $t = 0^+$ scales as $1/N^{1/2}$ according to (37). The contribution proportional to $\hat{N}_a - \hat{N}_b$ scales in the same way, since the total number difference $\approx N^{1/2}$ for the binomial distribution after the $\pi/2$ pulse. The same conclusion holds for the contribution proportional to \hat{D} , see (47). We reach the important conclusion that, for a finite time t in the thermodynamic limit,

$$\hat{\theta}_a - \hat{\theta}_b \approx \frac{1}{N^{1/2}} \quad (\text{D3})$$

As $\frac{N}{2} + \hat{F}$ is $O(N)$, it suffices to expand the exponential in (43) to first order included in the phase difference to obtain

$$\hat{S}_+ = \left[1 - i(\hat{\theta}_a - \hat{\theta}_b) + O\left(\frac{1}{N}\right) \right] \left(\frac{N}{2} + \hat{F}_R + i\hat{F}_I \right) \quad (\text{D4})$$

where we have split $\hat{F} = \hat{F}_R + i\hat{F}_I$ in terms of the hermitian operators \hat{F}_R and \hat{F}_I .

The antihermitian part of \hat{F} : The operator \hat{F}_I directly contributes to the antihermitian part of \hat{S}_+ , so it

has to be evaluated up to $\approx N^{1/2}$ included. Its exact expression is

$$\hat{F}_I = \frac{1}{2i} \sum_{\mathbf{r}} dV \left(\hat{\Lambda}_a^\dagger \hat{\Lambda}_b - \hat{\Lambda}_b^\dagger \hat{\Lambda}_a \right) = \frac{1}{2i} \sum_{\mathbf{k} \neq 0} \left(\hat{c}_{a\mathbf{k}}^\dagger \hat{c}_{b\mathbf{k}} - \text{h.c.} \right) \quad (\text{D5})$$

This corresponds to a complex scalar product between the bicomponent fields $(\hat{\Lambda}_a, \hat{\Lambda}_a^\dagger)$ and $(\hat{\Lambda}_b, \hat{\Lambda}_b^\dagger)$. The Bogoliubov equations of motion for spin state σ conserve this scalar product [31]. Due to the $a - b$ symmetry, the coefficient of Bogoliubov equations of motion are the same for the two internal states, and \hat{F}_I is a constant of motion within Bogoliubov theory. We can thus evaluate it at time 0^+ , taking into account the corrections to $\hat{c}_{\mathbf{k}\sigma}(0^+)$ due to the small condensate phase change induced by the pulse, as in (B4):

$$\hat{F}_I \simeq \frac{1}{2i} \sum_{\mathbf{k} \neq 0} (\hat{A}_{\mathbf{k}}^\dagger \hat{B}_{\mathbf{k}} - \hat{B}_{\mathbf{k}}^\dagger \hat{A}_{\mathbf{k}}) - \frac{1}{2} \left\{ \hat{y}, \frac{\hat{N}_{a\perp}^{(0)} - \hat{N}_{b\perp}^{(0)}}{\sqrt{\hat{N}_{a0}^{(0)}}} \right\} \quad (\text{D6})$$

where the operator \hat{y} is defined below (B3). This correction involving \hat{y} is important to ensure that $\langle \hat{S}_y^2(0^+) \rangle = N/4$ as it should be. The operator \hat{F}_I has a zero expectation value, this is why the same phenomenon as for the operator \hat{D} occurs. Calculating its variance, which is dominated by the contribution of the sum over \mathbf{k} in (D5),

$$\langle \hat{F}_I^2 \rangle = \frac{\langle \hat{N}_{a\perp}^{(0)} \rangle}{4} = \frac{1}{4} \sum_{\mathbf{k} \neq 0} V_{\mathbf{k}}^{(0)2} + n_{\mathbf{k}}^{(0)} [U_{\mathbf{k}}^{(0)2} + V_{\mathbf{k}}^{(0)2}] \quad (\text{D7})$$

we get as in (47) the estimate

$$\hat{F}_I \approx (N\epsilon_{\text{Bog}})^{1/2} \quad (\text{D8})$$

The hermitian part of \hat{F} : Contrarily to \hat{F}_I , the operator \hat{F}_R alone cannot contribute to the antihermitian part of \hat{S}_+ , it has to be multiplied at least once by the phase difference operator. To obtain \hat{S}_y up to $\approx N^{1/2}$ included, we thus need \hat{F}_R up to $\approx N$ included. To this end we decompose $\hat{N}_{\sigma 0}$ after the pulse, for $\sigma = a$ or b , as follows:

$$\hat{N}_{\sigma 0} = \frac{N}{2} + \delta\hat{N}_\sigma, \quad \delta\hat{N}_\sigma = \left(\hat{N}_\sigma - \frac{N}{2} \right) - \hat{N}_{\sigma\perp} \quad (\text{D9})$$

and we expand the square root in F (44) in the large N limit to obtain :

$$\sqrt{(\hat{N}_{a0} + 1)\hat{N}_{b0}} = \frac{N}{2} + \frac{1}{2}(1 + \delta\hat{N}_a + \delta\hat{N}_b) - \frac{(1 + \delta\hat{N}_a - \delta\hat{N}_b)^2}{4N} + \dots \quad (\text{D10})$$

In the second contribution in the right-hand side of (D10), we can replace $\hat{N}_a + \hat{N}_b$ with N . Since $\delta\hat{N}_a - \delta\hat{N}_b$

scales as $N^{1/2}$, the third contribution scales as N^0 and is thus negligible at the required order. The terms in the ... are of too high order in ϵ_{size} or in ϵ_{Bog} to be relevant. We conclude that, for our purposes, we can take

$$\hat{F}_R \simeq -\frac{1}{2} \sum_{\mathbf{r}} dV (\hat{\Lambda}_a^\dagger - \hat{\Lambda}_b^\dagger) (\hat{\Lambda}_a - \hat{\Lambda}_b) \quad (\text{D11})$$

By expanding the fields $\hat{\Lambda}_a$ and $\hat{\Lambda}_b$ over the Bogoliubov modes, we obtain \hat{F}_R in terms of the quasi-particle annihilation operators $\hat{c}_{\sigma\mathbf{k}}$ at time $t > 0$. Using (32) we can relate these operators to their value at time 0^+ , that we can replace by the leading order expression (38) to obtain

$$\hat{F}_R \simeq - \sum_{\mathbf{k} \neq 0} \left\{ V_k^2 + (U_k^2 + V_k^2) \hat{B}_{\mathbf{k}}^\dagger \hat{B}_{\mathbf{k}} + U_k V_k \left[e^{-2i\epsilon_k t/\hbar} \hat{B}_{\mathbf{k}} \hat{B}_{-\mathbf{k}} + \text{h.c.} \right] \right\} \quad (\text{D12})$$

Its expectation value is

$$\langle \hat{F}_R \rangle = - \sum_{\mathbf{k} \neq 0} 4U_k^2 V_k^2 \sin^2 \omega_k t \quad (\text{D13})$$

with $\omega_k = \epsilon_k/\hbar$. Even if the \hat{B} 's correspond to vacuum fluctuations, we still find (replacing the sum by an integral over \mathbb{R}^3 , which is convergent, and making the change of variable $\mathbf{k} = \mathbf{K}/\xi$, where ξ is the healing length) that $\langle \hat{F}_R \rangle/N$ scales as $(\rho a^3)^{1/2}$, which is $O(\epsilon_{\text{Bog}})$. For simplicity, we shall forget about this detail and consider that $\langle \hat{F}_R \rangle \approx N\epsilon_{\text{Bog}}$. Using Wick's theorem we have also determined the variance of \hat{F}_R ,

$$\text{Var } \hat{F}_R = \sum_{\mathbf{k} \neq 0} 8U_k^2 V_k^2 \sin^2 \omega_k t (1 + 4U_k^2 V_k^2 \sin^2 \omega_k t) \quad (\text{D14})$$

that scales as $N\epsilon_{\text{Bog}}$ (with the same subtlety) in the thermodynamic limit at finite times (it increases linearly with time). We summarize these estimates by the writing

$$\hat{F}_R \approx N\epsilon_{\text{Bog}} \pm (N\epsilon_{\text{Bog}})^{1/2} \quad (\text{D15})$$

As we said, we need to estimate \hat{F}_R up to $\approx N$ included. This means that the fluctuations of \hat{F}_R , that are $N^{1/2}$ times smaller, are negligible and the operator \hat{F}_R can be replaced by its mean value $\langle \hat{F}_R \rangle$.

Operators \hat{S}_y , etc: From the antihermitian part of (D4), and from the estimates (D3, D15, D8), we can approximate \hat{S}_y up to the terms $\approx N^{1/2}$ included as

$$\hat{S}_y \simeq \hat{F}_I - \frac{1}{2} \left\{ \hat{\theta}_a - \hat{\theta}_b, \frac{N}{2} + \langle \hat{F}_R \rangle \right\} \quad (\text{D16})$$

Squaring this expression, and neglecting terms of order larger than one in ϵ_{Bog} , we finally obtain the expectation value $\langle \hat{S}_y^2 \rangle/N$ with an accuracy up to $\approx \epsilon_{\text{size}}^0$ and $\approx \epsilon_{\text{Bog}}$ included, see (52). Taking the anticommutator of (D16) with \hat{S}_z and then the expectation value gives

(53), with the additional simplification that $\langle \hat{F}_I \hat{S}_z \rangle$ is purely imaginary and cancels out in the anticommutator [this results from (D1) and (D6), and in particular from $\langle \hat{y}\hat{x} \rangle = 1/(4i)$].

To conclude this Appendix, we give an expectation value useful for subsection IV C:

$$\langle \{\hat{S}_z, \hat{\mathcal{D}}\} \rangle = \sum_{\mathbf{k} \neq 0} s_k^2 \left(\langle \hat{A}_{\mathbf{k}}^\dagger \hat{A}_{\mathbf{k}} \rangle - V_k^2 \right) \quad (\text{D17})$$

where the $\hat{A}^\dagger \hat{A}$ expectation value is given by (C2).

Appendix E: With the oscillating terms in $\hat{\theta}_a - \hat{\theta}_b$

As announced above (35), we give here the analytical result for $\xi^2(t)$ (with the double expansion technique) without performing the approximation used in the main text of the paper. The temporally oscillating terms in the phase difference operator are now kept, which amounts to replacing $\hat{\mathcal{D}}$ in (35) with $\hat{\mathcal{D}}_{\text{tot}} = \hat{\mathcal{D}} + \hat{\mathcal{D}}_{\text{osc}}$ with the oscillating contribution

$$\hat{\mathcal{D}}_{\text{osc}}(t) = - \sum_{\mathbf{k} \neq 0} s_k^2 \frac{\sin \omega_k t}{\omega_k t} \left(e^{-i\omega_k t} \hat{A}_{\mathbf{k}} \hat{B}_{-\mathbf{k}} + \text{h.c.} \right) \quad (\text{E1})$$

where $\omega_k = \epsilon_k/\hbar$. In the renormalized time (59) one has also to replace $\hat{\mathcal{D}}$ with $\hat{\mathcal{D}}_{\text{tot}}$, which involves the new expectation value

$$\langle \{\hat{S}_z, \hat{\mathcal{D}}_{\text{osc}}\} \rangle = \sum_{\mathbf{k} \neq 0} s_k^2 \frac{\sin 2\omega_k t}{2\omega_k t} \left(\langle \hat{A}_{\mathbf{k}} \hat{A}_{-\mathbf{k}} \rangle + U_k V_k \right) \quad (\text{E2})$$

that will thus be added to the contribution (D17) [see (C2) for the $\hat{A}_{\mathbf{k}}^\dagger \hat{A}_{-\mathbf{k}}$ expectation value]. One can show that $t\langle \{\hat{S}_z, \hat{\mathcal{D}}_{\text{osc}}\} \rangle$ is uniformly bounded in time, so it contributes to τ as a time dependent small temporal shift. The result (60) is replaced by

$$\xi_{\text{tot}}^2(t) \simeq \frac{1 - 4\frac{\langle \hat{F}_R \rangle}{N}}{(\tau + \sqrt{1 + \tau^2})^2} + \frac{2 \left(\frac{\langle \hat{\mathcal{D}}_{\text{tot}}^2 \rangle}{N} \tau^2 + \frac{\langle \hat{F}_R \rangle}{N} + \zeta(t) \right)}{(\tau + \sqrt{1 + \tau^2}) \sqrt{1 + \tau^2}} \quad (\text{E3})$$

As expected, again, $\hat{\mathcal{D}}$ was replaced by $\hat{\mathcal{D}}_{\text{tot}}$. There is also an extra term, $\zeta(t)$, which is simply the value of the last term of (52) at time t minus its value at time 0^+ . This difference is no longer zero, because (56) no longer holds when $\hat{\mathcal{D}}$ is replaced with $\hat{\mathcal{D}}_{\text{tot}}$, since $\hat{\mathcal{D}}_{\text{tot}}$ has imaginary components. We find

$$N\zeta(t) = - \sum_{\mathbf{k} \neq 0} \sin^2 \omega_k t \frac{\rho g}{\hbar \omega_k} s_k^2 U_k^{(0)} V_k^{(0)} \left(n_k^{(0)} + \frac{1}{2} \right) \quad (\text{E4})$$

Note that $\zeta(t)$ is uniformly bounded in time, as $\langle \hat{F}_R \rangle/N$, it is thus not particularly relevant.

More significant deviations may come from the occurrence of $\langle \hat{\mathcal{D}}_{\text{tot}}^2 \rangle$ that differs from the original $\langle \hat{\mathcal{D}}^2 \rangle$ by the

two terms

$$\langle \{\hat{\mathcal{D}}, \hat{\mathcal{D}}_{\text{osc}}\} \rangle = \sum_{\mathbf{k} \neq 0} \frac{\sin 2\omega_k t}{2\omega_k t} \left(s_k^{(0)2} - \frac{s_k^8}{s_k^{(0)2}} \right) \left(n_k^{(0)} + \frac{1}{2} \right) \quad (\text{E5})$$

$$\langle \hat{\mathcal{D}}_{\text{osc}}^2 \rangle = \sum_{\mathbf{k} \neq 0} \left(\frac{\sin \omega_k t}{\omega_k t} \right)^2 s_k^4 \left[(U_k^2 + V_k^2) \langle \hat{A}_{\mathbf{k}}^\dagger \hat{A}_{\mathbf{k}} \rangle + U_k^2 - 2U_k V_k \langle \hat{A}_{\mathbf{k}} \hat{A}_{-\mathbf{k}} \rangle \cos 2\omega_k t \right] \quad (\text{E6})$$

These two terms however are $O(\epsilon_{\text{Bog}}/\tau^2)$ in the long time limit. At the relevant times $\tau \approx 1/\epsilon_{\text{Bog}}^{1/2}$, where the mul-

timode nature of the field starts limiting the squeezing, their contributions to ξ_{tot}^2 are $O(\epsilon_{\text{Bog}}^2)$ and negligible.

To summarize, the inclusion of the non-oscillating terms in the phase difference operator does not change at all the long time limit of ξ^2 (which, importantly, is its infimum in the Bogoliubov approximation): Eq. (61) is unchanged. At intermediate times, it gives small deviations. For the extreme case $k_B T/\rho g = 10$ and $(\rho a^3)^{1/2} = 10^{-3}$, where the non-condensed fraction reaches 10%, we find a maximal relative deviation of 2% between $\xi^2(t)$ of (60) and the more accurate $\xi_{\text{tot}}^2(t)$, at a time $\rho g t/\hbar \simeq 1.5$ when ξ^2 is still a factor $\simeq 4$ above its minimal value $\simeq 0.1$.

-
- [1] M. Kitagawa and M. Ueda. Squeezed spin states. *Phys. Rev. A*, 47(6):5138–5143, Jun 1993.
- [2] G. Santarelli, Ph. Laurent, P. Lemonde, A. Clairon, A. G. Mann, S. Chang, A. N. Luiten, and C. Salomon. Quantum projection noise in an atomic fountain: A high stability cesium frequency standard. *Phys. Rev. Lett.*, 82(23):4619–4622, Jun 1999.
- [3] D. J. Wineland, J. J. Bollinger, W. M. Itano, and D. J. Heinzen. Squeezed atomic states and projection noise in spectroscopy. *Phys. Rev. A*, 50(1):67–88, Jul 1994.
- [4] Sorensen A., Duan L.M., Cirac J.I., and Zoller P. Many-particle entanglement with Bose-Einstein condensates. *Nature*, 409:63, 2001.
- [5] Ian D. Leroux, Monika H. Schleier-Smith, and Vladan Vuletić. Implementation of cavity squeezing of a collective atomic spin. *Phys. Rev. Lett.*, 104(7):073602, Feb 2010.
- [6] C. Gross, T. Zibold, E. Nicklas, J. Esteve, and Oberthaler M.K. Nonlinear atom interferometer surpasses classical precision limit. *Nature*, 464:1165, 2010.
- [7] Riedel M.F., Boehi P., Li Yun, Hansch T.W., Sinatra A., and Treutlein P. Atom-chip-based generation of entanglement for quantum metrology. *Nature*, 464:1170, 2010.
- [8] Yun Li, Y. Castin, and A. Sinatra. Optimum spin-squeezing in Bose-Einstein condensates with particle losses. *Phys. Rev. Lett.*, 100:210401, 2008.
- [9] A. Sinatra, E. Witkowska, J.-C. Dornstetter, Yun Li, and Y. Castin. Limit to spin squeezing in finite temperature Bose-Einstein condensates. *Phys. Rev. Lett.*, 2011.
- [10] G. Ferrini, D. Spehner, A. Minguzzi, and F. W. J. Hekking. Effect of phase noise on useful quantum correlations in Bose Josephson junctions. *Phys. Rev. A*, 84:043628, Oct 2011.
- [11] A Sinatra, J.C. Dornstetter, and Y Castin. Spin squeezing in Bose-Einstein condensates: Limits imposed by decoherence. *arXiv:1109.2401*.
- [12] Vladan et al. Vuletic. Unitary cavity spin squeezing by quantum erasure. *arXiv:1109.3752*.
- [13] Yvan Castin and Jean Dalibard. Relative phase of two Bose-Einstein condensates. *Phys. Rev. A*, 55:4330–4337, Jun 1997.
- [14] A. Sinatra and Y. Castin. Phase dynamics of Bose-Einstein condensates: Losses versus revivals. *Eur. Phys. Jour. B*, 4:247, 1998.
- [15] A. B. Kuklov and Joseph L. Birman. Orthogonality catastrophe and decoherence of a confined Bose-Einstein condensate at finite temperature. *Phys. Rev. A*, 63(1):013609, Dec 2000.
- [16] A. Sinatra, Y. Castin, and E. Witkowska. Nondiffusive phase spreading of a Bose-Einstein condensate at finite temperature. *Phys. Rev. A*, 75(3):033616, Mar 2007.
- [17] A. Sinatra and Y. Castin. Genuine phase diffusion of a Bose-Einstein condensate in the microcanonical ensemble: A classical field study. *Phys. Rev. A*, 78(5):053615, Nov 2008.
- [18] A. Sinatra, Y. Castin, and E. Witkowska. Coherence time of a Bose-Einstein condensate. *Phys. Rev. A*, 80(3):033614, Sep 2009.
- [19] Uffe V. Poulsen and Klaus Mølmer. Positive-P simulations of spin squeezing in a two-component Bose condensate. *Phys. Rev. A*, 64(1):013616, Jun 2001.
- [20] Anders Søndberg Sørensen. Bogoliubov theory of entanglement in a Bose-Einstein condensate. *Phys. Rev. A*, 65(4):043610, Apr 2002.
- [21] Y. Kagan, B.V. Svistunov, and G.V. Shlyapnikov. Kinetics of Bose-Einstein condensation in an interacting Bose gas. *Sov. Phys. JETP*, 75:387, 1992.
- [22] Kedar Damle, Satya N. Majumdar, and Subir Sachdev. Phase ordering kinetics of the Bose gas. *Phys. Rev. A*, 54:5037, 1996.
- [23] Krzysztof Goral, Mariusz Gajda, and Kazimierz Rzążewski. Multi-mode description of an interacting Bose-Einstein condensate. *Optics Express*, 8:92, 2001.
- [24] M. J. Davis, S. A. Morgan, and K. Burnett. Simulations of Bose fields at finite temperature. *Phys. Rev. Lett.*, 87:160402, 2001.
- [25] Carlos Lobo, Alice Sinatra, and Yvan Castin. Vortex lattice formation in Bose-Einstein condensates. *Phys. Rev. Lett.*, 92:020403, 2004.
- [26] M. J. Steel, M. K. Olsen, L. I. Plimak, P. D. Drummond, S. M. Tan, M. J. Collett, D. F. Walls, and R. Graham. Dynamical quantum noise in trapped Bose-Einstein condensates. *Phys. Rev. A*, 58:4824, 1998.
- [27] A. Sinatra, Y. Castin, and C. Lobo. A Monte Carlo formulation of the Bogolubov theory. *Journal of Modern Optics*, 47:2629, 2000.
- [28] A. Sinatra, C. Lobo, and Y. Castin. Classical-field method for time dependent Bose-Einstein condensed gases. *Phys. Rev. Lett.*, 87:210404, 2001.
- [29] A. Sinatra, C. Lobo, and Y. Castin. The truncated Wigner method for Bose condensed gases: limits of validity and applications. *J. Phys. B*, 35:3599, 2002.

- [30] Pricoupenko L. and Castin Y. Three fermions in a box at the unitary limit: universality in a lattice model. *J. Phys. A*, 40:12863, 2007.
- [31] Y. Castin and R. Dum. Low-temperature Bose-Einstein condensates in time-dependent traps: Beyond the $U(1)$ symmetry-breaking approach. *Phys. Rev. A*, 57(4):3008–3021, Apr 1998.
- [32] M. Girardeau and R. Arnowitt. Theory of many-boson systems: Pair theory. *Phys. Rev.*, 113:755–761, Feb 1959.
- [33] Carruthers P. and Nieto M. Phase and angle variables in quantum mechanics. *Rev. Mod. Phys.*, 40:411, 1968.
- [34] C. W. Gardiner. Particle-number-conserving Bogoliubov method which demonstrates the validity of the time-dependent Gross-Pitaevskii equation for a highly condensed Bose gas. *Phys. Rev. A*, 56:1414–1423, Aug 1997.
- [35] S Giorgini. *Phys. Rev. A*, 57:2949, 1998.
- [36] In ^{87}Rb atoms this may be done by spatial separation of the spin states [7] or by Feshbach tuning of the a - b scattering length [6].
- [37] The exact relation between the bare coupling constant and the effective coupling constant is $1/g = 1/g_0 + \int_{\text{FBZ}} \frac{d^3k}{(2\pi)^3} \frac{m}{\hbar^2 k^2}$, where $\text{FBZ} = [-\pi/l, \pi/l]^3$.
- [38] In this classical limit, the substitution $g_0 \rightarrow g$ is required, since the difference between $1/g_0$ and $1/g$ is due to quantum fluctuations.
- [39] In the classical field simulations, to ensure maximal ergodicity, we did not use a cubic lattice. We used the following aspect ratios for the quantization box, $L_x^2 : L_y^2 : L_z^2 = \sqrt{2} : (1 + \sqrt{5})/2 : \sqrt{3}$, and we discretized the positions with the same even number of points n_{max} along each direction. This corresponds in condition (16) to a slightly asymmetric FBZ.
- [40] In our simulations (with finite size systems) we increase N and decrease g while V , T and Ng are fixed.